

Enhanced photodegradation of dimethoxybenzene isomers in/on ice compared to in aqueous solution

Ted Hullar, Theo Tran, Zekun Chen, Fernanda Bononi, Oliver Palmer, Davide Donadio, and Cort Anastasio

Contents

Supplemental Section S1. Details of light absorption modeling.....	1
Supplemental Table S1. Experimental light intensity correction factors.....	2
Supplemental Table S2. Light absorbance values.....	3
Supplemental Table S3. Illumination experiment measured parameters.....	10
Supplementary Table S4. Rate constants for light absorption.....	11
Supplemental Table S5. Machine learning training and testing errors.....	11
Supplemental Figures S1a-S12h. Results for individual illumination experiments.....	25
Supplemental Figure S13. Experimental and modeled photon fluxes.....	26
Supplemental Figure S14. Light absorbance spectra for DMOB isomers.....	27
Supplemental Figure S15. Linear decomposition analysis for DMOB isomers.....	28
Supplemental Figure S16. Action spectra for DMOB light absorbance.....	30
Supplemental Figure S17. Photodegradation rate constant ratios for shifted absorbance curves.....	31
Supplemental Figure S18. Guaiacol photodegradation rate constants for various illumination conditions.....	32
Supplemental Figure S19. Absorbance spectra for DMOBs compared to assumed Gaussian peaks.....	33
Supplemental Figure S20. Model compound absorbance spectra for various peak locations.....	34
Supplemental Figure S21. Model compound photodegradation rate constants for various peak locations.....	35
Supplemental Figure S22. Model compound absorbance spectra for various peak widths.....	36
Supplemental Figure S23. Model compound photodegradation rate constants for various peak widths.....	37
Supplemental Figure S24. Model compound absorbance spectra for various molar absorptivities.....	38
Supplemental Figure S25. Model compound photodegradation rate constant for various molar absorptivities.....	39
Supplemental Figure S26. Machine learning parity plots.....	40
References.....	40

Supplemental Section S1. Details of light absorption modeling

Justification for a single machine learning model for all three DMOB isomers. As shown in Supplemental Figure S26 and Supplemental Table S5, the machine learning (ML) model achieves a training R^2 of 0.981 and a testing R^2 of 0.965, along with a training mean absolute error (MAE) of 1.42 nm and a testing MAE of 1.88 nm. Since a universal ML model is fitted to predict the vertical excitation wavelengths (λ) for all three DMOB isomers, we broke down the overall MAE to assess the ML model performance for each molecule. As shown in Supplemental Table S5, the negligible variations in the MAE implies that our model can generate predictions

with no bias towards a particular molecule. This trend justified our approach to predict excitation wavelengths for all three molecules using only one ML model. Meanwhile, the overall training and testing MAE for DMOB isomers, as well as the average testing MAE for molecules in solution (1.93 ± 0.16 nm) and at the air-ice interface (1.82 ± 0.23 nm), suggest that this model can be generalized to predict excitation wavelengths for all three isomers in both solution and at the air-ice interface.

Additional information for hyperparameters used to compute Bispectrum Component (BC). Before describing the atomic environment for the three DMOB isomers using a bispectrum component, a set of hyperparameters must be carefully defined. First, the cut-off radius for hydrogen, carbon and oxygen ($R_{cut,H}$, $R_{cut,C}$ & $R_{cut,O}$) are set to 1.5, 2.5, and 3 Å respectively, which corresponds to approximately second-neighbor distances. Meanwhile, to reflect the relative importance for the chemical environment with respect to each atom type, the dimensionless weight factors (ω_H , ω_C & ω_O) of 1.0, 2.0, and 3.0 are set accordingly. Lastly, to ensure a sufficiently large initial feature space for the LASSO model development, a $2j_{max}$ parameter is chosen to be 14, which results in a total of 858 bispectrum components.

Formulation of linear decomposition analysis. To pinpoint the relative importance to the predictions of λ with respect to functional groups of DMOB isomers, a linear decomposition analysis can be performed and formulated as:

$$\lambda_{predicted} = \lambda_0 + \lambda_{predicted,OCH_3} + \lambda_{predicted,C_6H_4}$$

$$\lambda_{Decomposed} = \frac{(\lambda_{predicted,OCH_3} + \lambda_{predicted,C_6H_4})}{\lambda_{predicted} - \lambda_0}$$

In the above equation, λ_0 is the intercept of the LASSO model; $\lambda_{predicted,OCH_3}$ and $\lambda_{predicted,C_6H_4}$ represent predictions contributions from the methoxy groups and from the phenyl ring; and $\lambda_{Decomposed}$ is defined to express the decomposition with respect to the functional groups by percentage.

Supplemental Table S1. Experimental light intensity correction factors. Light intensity correction factors for the experimental illumination system, determined as the ratio of aqueous j_{2NB} in a given position divided by the corresponding value in the reference position (B2). These factors were used to normalize photodegradation rates to the photon flux in each position. Illuminated samples were put in columns B and C, while dark samples (which were uncorrected for photon flux) were placed in columns A and D.

		Column			
		A	B	C	D
Row	1	0.18	1.00	0.80	0.55
	2	0.44	1.00	0.83	0.89
	3	0.61	1.06	0.99	1.10
	4	0.18	1.08	0.95	0.77

Supplemental Table S2. Light absorbance values. Measured, predicted, and modeled light absorbance values for a) 1,2-, b) 1,3-, and c) 1,4-DMOB. Molar absorptivities (columns 2 and 3) were measured for aqueous and predicted for the air-ice interface. Modeled absorbance values (columns 4 and 5) were computed using molecular modeling techniques. See footnotes and text for details.

a) 1,2-Dimethoxybenzene

Modeled parameters used to predict air-ice interface spectrum:

Peak wavelength shift from aqueous to air-ice interface: 2.4 nm

Peak height ratio, air-ice interface / aqueous: 1.17

Peak width ratio, air-ice interface / aqueous: 0.94

Wavelength (nm)	Molar absorptivity ($M^{-1} cm^{-1}$)		Modeled absorbance (AU) ^c	
	Aqueous (measured) ^a	Air-ice interface (predicted) ^b	Aqueous	Air-ice interface
250	519	0	0	0
251	572	0	0	0
252	631	0	0	0
253	707	0	0	0
254	795	613	0	0
255	897	682	0	0
256	1010	765	0	0
257	1132	857	0	0
258	1272	975	0	0
259	1422	1113	0	0
260	1585	1250	0	0
261	1760	1424	0	0
262	1950	1610	0	0
263	2153	1794	0	0
264	2349	2019	0	0
265	2571	2258	0.003	0
266	2745	2497	0.008	0
267	2909	2749	0.017	0.001
268	3070	3033	0.031	0.005
269	3236	3233	0.059	0.016
270	3383	3445	0.091	0.037
271	3490	3657	0.150	0.077
272	3564	3843	0.236	0.112
273	3610	4019	0.367	0.155
274	3594	4134	0.556	0.263
275	3498	4219	0.755	0.439
276	3337	4227	1.022	0.632
277	3196	4133	1.375	0.813
278	3109	3958	1.662	1.026
279	3043	3772	1.859	1.276
280	2883	3641	2.050	1.552
281	2486	3566	2.096	1.886
282	1960	3373	2.008	2.137

283	1415	2846	1.995	2.273
284	978	2229	1.994	2.386
285	649	1549	1.843	2.452
286	434	1014	1.612	2.422
287	284	677	1.410	2.260
288	186	426	1.240	2.014
289	117	271	1.035	1.753
290	75	174	0.823	1.459
291	47	105	0.623	1.167
292	30	63	0.439	0.937
293	19	40	0.301	0.717
294	12	24	0.211	0.477
295	8.17	15	0.147	0.296
296	5.35	10	0.098	0.202
297	3.40	6.26	0.072	0.156
298	2.15	3.81	0.065	0.116
299	1.37	2.42	0.056	0.072
300	0.87	1.47	0.040	0.046
301	0.55	0.89	0.028	0.031
302	0.35	0.57	0.022	0.016
303	0.22	0.34	0.017	0.005
304	0.14	0.21	0.011	0.001
305	0.089	0.13	0.005	0
306	0.057	0.080	0.002	0
307	0.036	0.048	0.000	0
308	0.023	0.031	0.001	0
309	0.014	0.019	0.004	0
310	0.0092	0.011	0.005	0
311	0.0058	0.0072	0.003	0
312	0.0037	0.0043	0.001	0
313	0.0023	0.0026	0	0
314	0.0015	0.0017	0	0
315	0.00094	0.0010	0	0
316	0.00060	0.00062	0	0

b) 1,3-Dimethoxybenzene

Modeled parameters used to predict air-ice interface spectrum:

Peak wavelength shift from aqueous to air-ice interface: 5.2 nm

Peak height ratio, air-ice interface / aqueous: 0.91

Peak width ratio, air-ice interface / aqueous: 1.27

Wavelength (nm)	Molar absorptivity ($M^{-1} cm^{-1}$)		Modeled absorbance (AU) ^c	
	Aqueous (measured) ^a	Air-ice interface (predicted) ^b	Aqueous	Air-ice interface
250	536	522	0	0
251	600	571	0	0
252	670	626	0	0
253	758	690	0	0

254	853	758	0	0
255	967	836	0	0
256	1098	925	0	0
257	1235	1023	0	0
258	1395	1111	0	0
259	1558	1225	0	0
260	1745	1343	0	0
261	1938	1464	0	0.001
262	2158	1606	0.002	0.004
263	2393	1747	0.008	0.005
264	2570	1903	0.012	0.004
265	2796	2070	0.027	0.006
266	2984	2215	0.066	0.015
267	3165	2339	0.122	0.024
268	3322	2504	0.160	0.040
269	3494	2646	0.226	0.084
270	3663	2780	0.356	0.127
271	3859	2914	0.510	0.139
272	3997	3023	0.624	0.192
273	4010	3148	0.789	0.288
274	3889	3272	1.035	0.422
275	3638	3407	1.258	0.579
276	3443	3526	1.423	0.725
277	3385	3627	1.582	0.843
278	3476	3653	1.683	0.986
279	3479	3607	1.742	1.179
280	3190	3470	1.718	1.315
281	2592	3290	1.592	1.422
282	1867	3149	1.513	1.505
283	1260	3091	1.464	1.551
284	844	3112	1.318	1.570
285	541	3178	1.109	1.586
286	348	3166	0.903	1.590
287	224	2976	0.741	1.545
288	142	2603	0.595	1.439
289	89	2076	0.454	1.276
290	56	1584	0.347	1.140
291	36	1147	0.254	1.020
292	22	839	0.183	0.884
293	13	586	0.130	0.755
294	8.3	433	0.095	0.648
295	5.3	304	0.067	0.545
296	2.9	213	0.040	0.432
297	1.8	150	0.023	0.346
298	1.2	104	0.016	0.280
299	0.72	71	0.015	0.223
300	0.45	49	0.012	0.189
301	0.28	34	0.007	0.159

302	0.18	23	0.003	0.122
303	0.11	16	0.001	0.087
304	0.069	11	0	0.061
305	0.043	7.5	0	0.044
306	0.027	5.2	0	0.036
307	0.017	3.4	0	0.029
308	0.011	2.2	0	0.021
309	0.0067	1.5	0	0.016
310	0.0042	1.0	0	0.013
311	0.0026	0.73	0	0.010
312	0.0016	0.52	0	0.006
313	0.0010	0.36	0	0.003
314	0.00064	0.25	0	0.002
315	0.00040	0.17	0	0.002
316	0	0.12	0	0.001
317	0	0.080	0	0
318	0	0.055	0	0
319	0	0.038	0	0
320	0	0.026	0	0
321	0	0.019	0	0
322	0	0.013	0	0
323	0	0.0089	0	0
324	0	0.0061	0	0
325	0	0.0042	0	0
326	0	0.0029	0	0
327	0	0.0020	0	0
328	0	0.0014	0	0
329	0	0.00093	0	0
330	0	0.00068	0	0
331	0	0.00046	0	0
332	0	0.00015	0	0

c) 1,4-Dimethoxybenzene

Modeled parameters used to predict air-ice interface spectrum:

Peak wavelength shift from aqueous to air-ice interface: 1.6 nm

Peak height ratio, air-ice interface / aqueous: 1.06

Peak width ratio, air-ice interface / aqueous: 0.92

Wavelength (nm)	Molar absorptivity ($M^{-1} cm^{-1}$)		Modeled absorbance (AU) ^c	
	Aqueous (measured) ^a	Air-ice interface (predicted) ^b	Aqueous	Air-ice interface
250	167	0	0	0
251	163	0	0	0
252	165	0	0	0
253	171	0	0	0
254	181	0	0	0
255	197	176	0	0
256	216	174	0	0

257	238	178	0	0
258	267	187	0	0
259	298	201	0	0
260	336	222	0	0
261	379	247	0	0
262	428	280	0	0
263	482	316	0	0
264	540	361	0	0
265	603	411	0	0
266	667	471	0	0
267	739	536	0	0
268	819	602	0	0
269	895	681	0	0
270	975	760	0	0
271	1060	843	0	0
272	1149	933	0	0
273	1244	1025	0	0
274	1341	1124	0	0
275	1446	1227	0	0
276	1552	1338	0	0
277	1655	1456	0	0
278	1755	1581	0	0
279	1851	1696	0	0
280	1947	1820	0.002	0
281	2026	1932	0.002	0
282	2119	2044	0.001	0
283	2192	2131	0.000	0
284	2251	2236	0.002	0
285	2302	2324	0.006	0
286	2321	2393	0.009	0
287	2326	2441	0.016	0
288	2314	2469	0.024	0
289	2276	2466	0.036	0
290	2221	2434	0.053	0.002
291	2150	2380	0.081	0.008
292	2072	2305	0.114	0.014
293	1983	2214	0.137	0.018
294	1875	2110	0.181	0.028
295	1761	2000	0.275	0.066
296	1633	1867	0.379	0.132
297	1472	1714	0.475	0.211
298	1301	1525	0.577	0.312
299	1114	1320	0.700	0.428
300	917	1093	0.866	0.551
301	727	870	1.068	0.716
302	554	662	1.302	0.917
303	415	482	1.528	1.133
304	303	345	1.683	1.381

305	221	242	1.784	1.601
306	157	166	1.885	1.798
307	109	115	1.993	1.990
308	74	76	2.034	2.086
309	52	51	1.959	2.131
310	35	33	1.788	2.145
311	25	22	1.610	2.058
312	17	16	1.486	1.883
313	13	11	1.361	1.654
314	8.8	7.22	1.204	1.418
315	6.1	4.83	1.039	1.216
316	4.2	3.22	0.873	1.048
317	2.9	2.15	0.713	0.873
318	2.0	1.44	0.560	0.701
319	1.4	1.00	0.421	0.550
320	1.0	0.67	0.309	0.415
321	0.67	0.45	0.225	0.296
322	0.47	0.30	0.166	0.199
323	0.32	0.20	0.124	0.139
324	0.22	0.13	0.085	0.104
325	0.16	0.089	0.053	0.073
326	0.11	0.059	0.032	0.047
327	0.075	0.040	0.017	0.030
328	0.052	0.026	0.010	0.018
329	0.036	0.018	0.006	0.010
330	0.025	0.012	0.004	0.007
331	0.017	0.0082	0.003	0.005
332	0.012	0.0055	0.002	0.002
333	0.0083	0.0037	0.001	0.001
334	0.0057	0.0024	0	0
335	0.0040	0.0016	0	0
336	0.0028	0.0011	0	0
337	0.0019	0.00073	0	0
338	0.0013	0.00049	0	0
339	0.00092	0	0	0
340	0.00064	0	0	0
341	0.00044	0	0	0

^a For each DMOB, we measured absorbance spectra in five aqueous solutions (10-1000 μM) at 25 °C using a UV-2501PC spectrophotometer (Shimadzu) in 1.0 cm cuvettes against a MQ reference cell. For each wavelength, we calculated the base-10 molar absorptivity as the slope of the linear regression of measured absorbance versus the DMOB concentration. At wavelengths at and above 296, 296, and 313 nm for 1,2-, 1,3-, and 1,4-DMOB, respectively, calculated molar absorptivities were $< 5 \text{ M}^{-1} \text{ cm}^{-1}$ and very noisy. To better estimate molar absorptivities in these ranges, we used the measured data from 290-296, 290-296, and 307-313 nm for each compound, respectively, plotted $\ln(\epsilon_{\text{DMOB},\lambda})$ vs λ , then used the slope of the linear regression to determine $\epsilon_{\text{DMOB},\lambda}$ at wavelengths longer than these three ranges.

^b Predicted base-10 molar absorptivities at the air-ice interface, based on aqueous absorbance values adjusted using modeled absorbance changes between solution and the air-ice interface. See text for details.

^c Results of computationally-determined absorbance spectra in aqueous solution and at the air-ice interface in arbitrary absorbance units. See text for details.

Supplemental Table S3. Illumination experiment measured parameters. Summary of parameters determined from illumination experiments, summarized for each DMOB isomer and experimental condition. “avg” represents the mean value for each isomer and sample treatment, “SD” is the standard deviation, and “95% CI” is the 95 percent confidence interval of the mean.

	n ^a	$j_{\text{DMOB}} (\text{min}^{-1})^{\text{b}}$			$k'_{\text{DMOB, dark}} (\text{min}^{-1})^{\text{c}}$			$j_{\text{DMOB, exp}} (\text{min}^{-1})^{\text{d}}$			$j^*_{\text{DMOB}} (\text{min}^{-1}/\text{s}^{-1})^{\text{e}}$			$j_{2\text{NB}} (\text{s}^{-1})^{\text{f}}$		
		avg	SD	95% CI	avg	SD	95% CI	avg	SD	95% CI	avg	SD	95% CI	avg	SD	95% CI
<u>1,2-DMOB</u>																
Aqueous	3	9.3E-06	4.7E-06	1.2E-05	3.5E-06	2.2E-06	5.5E-06	5.8E-06	3.1E-06	7.8E-06	1.9E-03	1.1E-03	2.7E-03	3.2E-03	2.7E-04	6.6E-04
Freezer frozen solution	3	-4.8E-06	2.9E-05	7.1E-05	-4.9E-05	1.6E-05	3.9E-05	-4.8E-06	2.9E-05	7.1E-05	-1.5E-03	9.9E-03	2.5E-02	2.9E-03	1.8E-04	4.5E-04
Liquid nitrogen frozen solution	4	5.0E-06	7.8E-06	1.2E-05	-1.1E-06	2.8E-06	4.4E-06	4.5E-06	7.9E-06	1.3E-05	1.9E-03	3.4E-03	5.4E-03	2.6E-03	1.9E-04	3.0E-04
Vapor-deposited to ice surface	3	1.8E-04	1.7E-04	4.2E-04	2.1E-05	2.3E-05	5.7E-05	1.5E-04	1.6E-04	4.0E-04	2.9E-02	2.2E-02	5.5E-02	5.2E-03	2.6E-03	6.5E-03
Vapor-deposited to snow	5	4.3E-05	1.5E-05	1.9E-05	-2.1E-06	2.8E-05	3.5E-05	3.3E-05	9.9E-06	1.2E-05	2.7E-02	8.4E-03	1.0E-02	1.2E-03	3.1E-05	3.9E-05
<u>1,3-DMOB</u>																
Aqueous	6	1.1E-05	1.0E-05	1.1E-05	1.5E-05	1.4E-05	1.5E-05	-3.4E-06	9.1E-06	9.5E-06	-1.1E-03	2.9E-03	3.0E-03	3.3E-03	2.1E-04	2.2E-04
Freezer frozen solution	0															
Liquid nitrogen frozen solution	3	2.8E-05	7.9E-06	2.0E-05	-1.1E-07	2.3E-06	5.7E-06	2.8E-05	9.0E-06	2.2E-05	1.3E-02	4.2E-03	1.1E-02	2.1E-03	3.8E-05	9.6E-05
Vapor-deposited to ice surface	0															
Vapor-deposited to snow	5	2.2E-04	5.1E-05	6.3E-05	1.6E-04	3.7E-05	4.6E-05	6.2E-05	4.9E-05	6.1E-05	5.4E-02	4.5E-02	5.6E-02	1.2E-03	7.4E-05	9.2E-05
<u>1,4-DMOB</u>																
Aqueous	3	2.0E-05	6.3E-06	1.6E-05	7.1E-06	6.0E-06	1.5E-05	1.3E-05	2.7E-06	6.7E-06	4.3E-03	7.3E-04	1.8E-03	3.1E-03	1.2E-04	3.0E-04
Freezer frozen solution	0															
Liquid nitrogen frozen solution	3	4.5E-05	3.4E-06	8.5E-06	-2.3E-07	8.2E-06	2.0E-05	4.3E-05	6.2E-06	1.5E-05	1.5E-02	3.6E-03	9.0E-03	3.0E-03	5.2E-04	1.3E-03
Vapor-deposited to ice surface	5	1.1E-04	7.1E-05	8.8E-05	5.5E-05	4.7E-05	5.9E-05	5.2E-05	9.5E-05	1.2E-04	1.4E-02	2.5E-02	3.1E-02	4.2E-03	5.6E-04	6.9E-04
Vapor-deposited to snow	8	4.2E-04	2.7E-04	2.2E-04	2.2E-04	2.4E-04	2.0E-04	2.0E-04	1.7E-04	1.4E-04	1.1E-01	9.1E-02	7.6E-02	1.6E-03	6.9E-04	5.8E-04

^a Number of experiments

^b The pseudo-first-order rate constant for DMOB loss during sample illumination, obtained as the slope of $\ln([\text{DMOB}]_t/[\text{DMOB}]_0)$ vs t , where $[\text{DMOB}]_t$ was corrected for variations in light flux at each illumination position

^c Rate constant for DMOB loss in dark controls

^d Dark-corrected experimental photodegradation rate constant, obtained by subtracting $k'_{\text{DMOB, dark}}$ from j_{DMOB}

^e Photon flux-normalized photodegradation rate constant, normalized by dividing the dark-corrected experimental photodegradation rate constant ($j_{\text{DMOB, exp}}$) by the daily measured $j_{2\text{NB}}$ value

^f Daily measured 2NB photolysis rate constant, measured using the same sample preparation method as the DMOB sample, except in the case of snow samples. For snow samples, $j_{2\text{NB}}$ was measured in aqueous solution and multiplied by previously determined correction factor of 0.38 to give a snow $j_{2\text{NB}}$ value

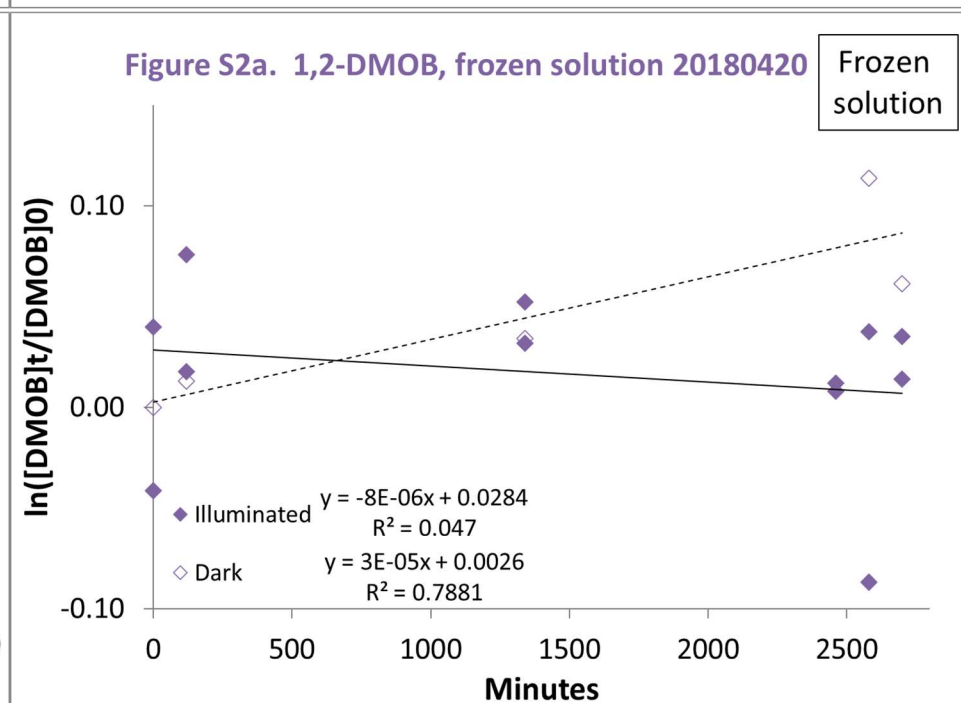
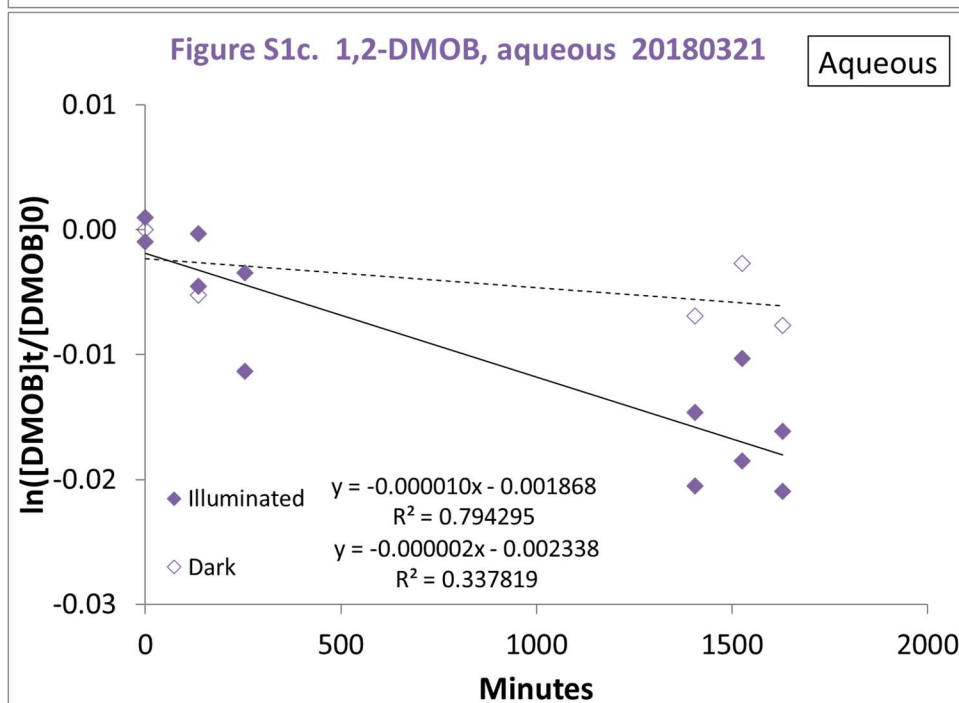
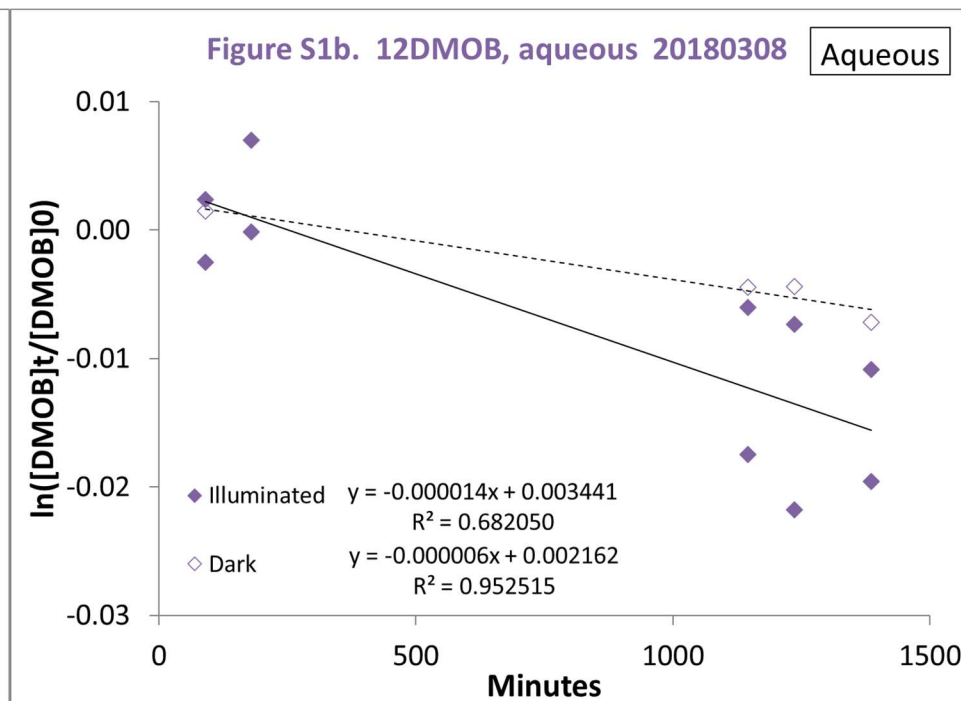
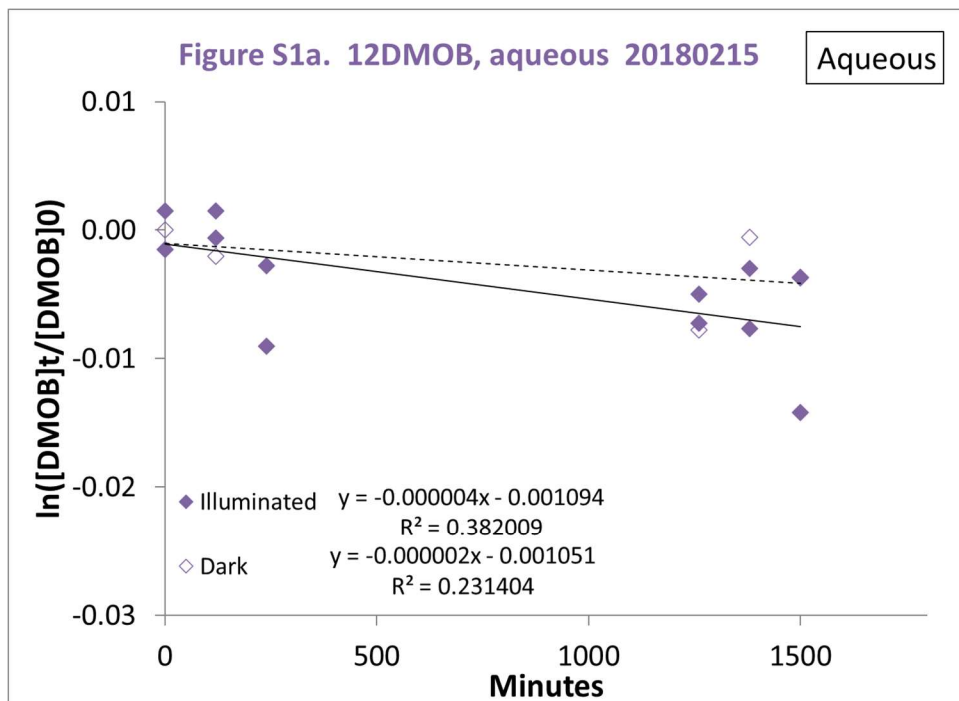
Supplementary Table S4. Rate constants for light absorption. Integrated rate constants for light absorption, determined for each DMOB isomer by multiplying the measured (aqueous) or predicted (air-ice interface) molar absorptivity by the experimental or Summit conditions photon flux, then summing the resulting values. Ratios for each isomer are the air-ice interface rate constant divided by the aqueous rate constant.

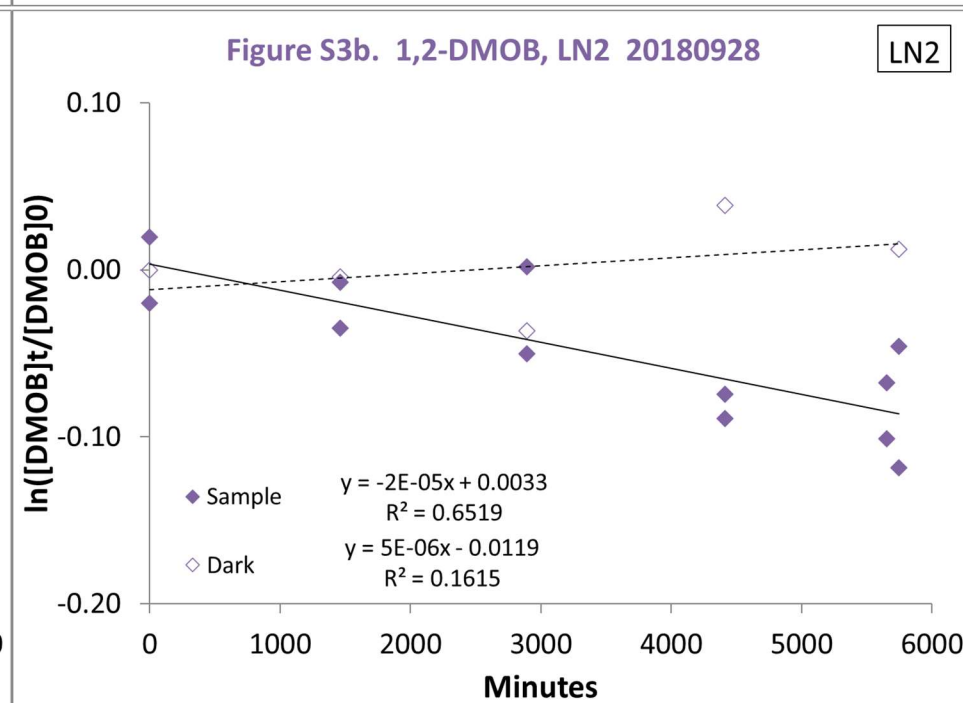
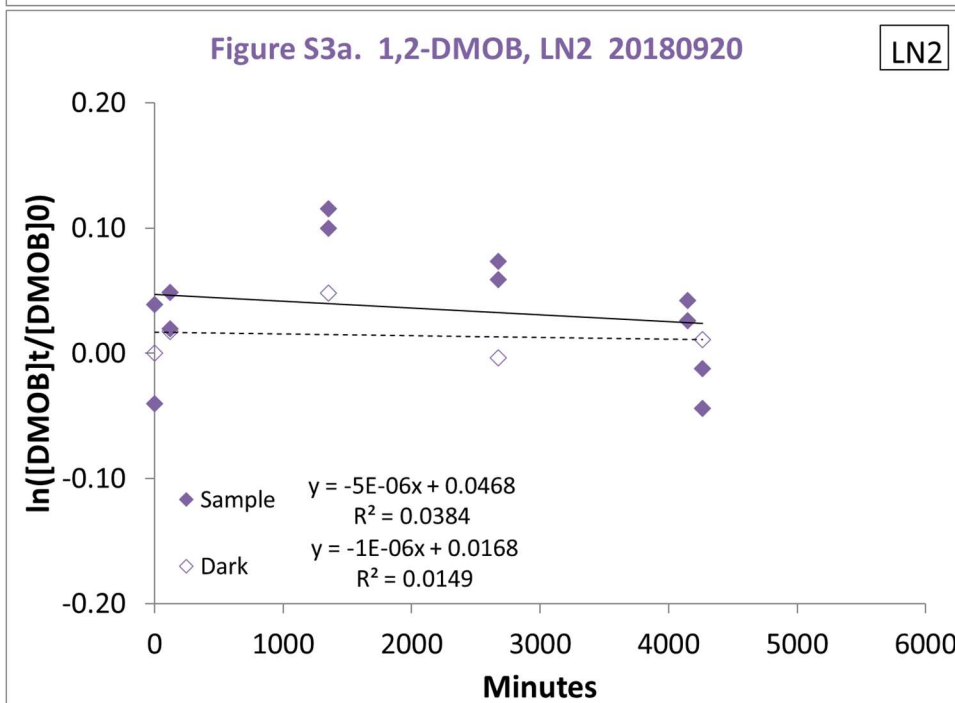
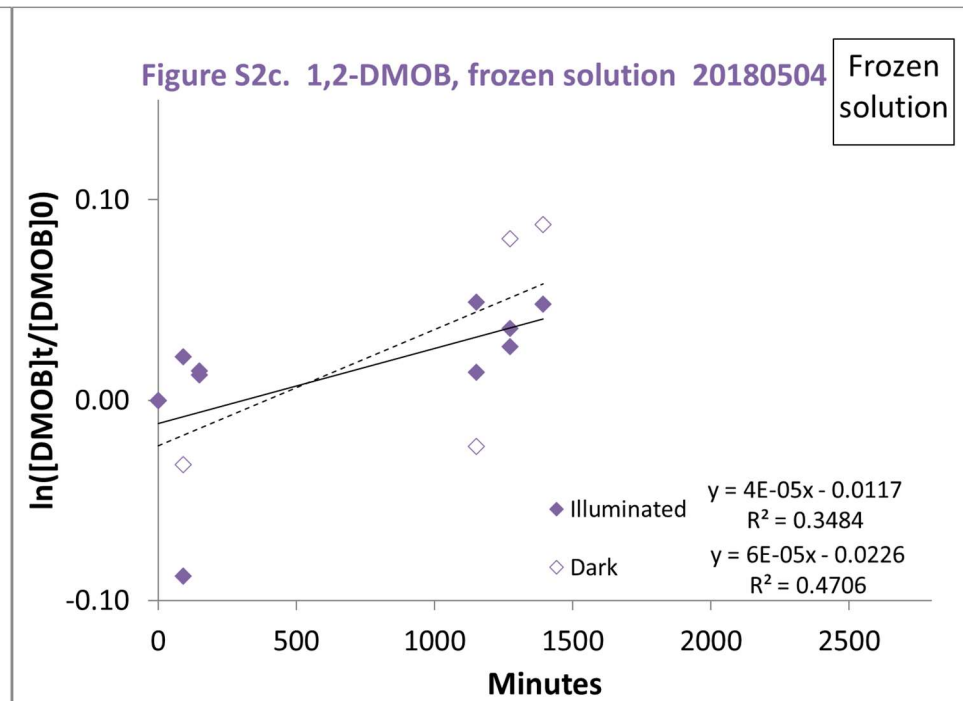
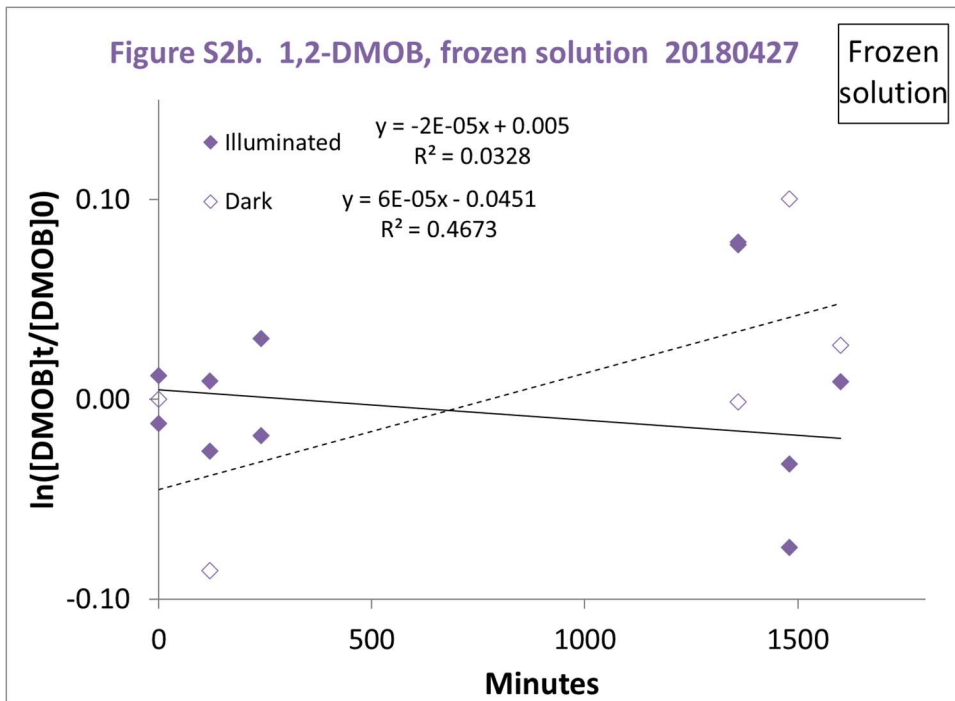
Compound	Experimental light conditions			Summit light conditions		
	Rate constant for light absorption ^a (photons molecule ⁻¹ s ⁻¹)		Rate constant ratio Air-ice interface/ aqueous	Rate constant for light absorption ^a (photons molecule ⁻¹ s ⁻¹)		Rate constant ratio Air-ice interface/ aqueous
	Aqueous	Air-ice interface		Aqueous	Air-ice interface	
1,2-DMOB	6.8E-06	1.2E-05	1.7	3.4E-08	5.1E-08	1.5
1,3-DMOB	6.5E-06	3.4E-05	5.3	1.7E-08	2.8E-06	170
1,4-DMOB	1.0E-04	1.2E-04	1.1	8.1E-05	8.3E-05	1.0

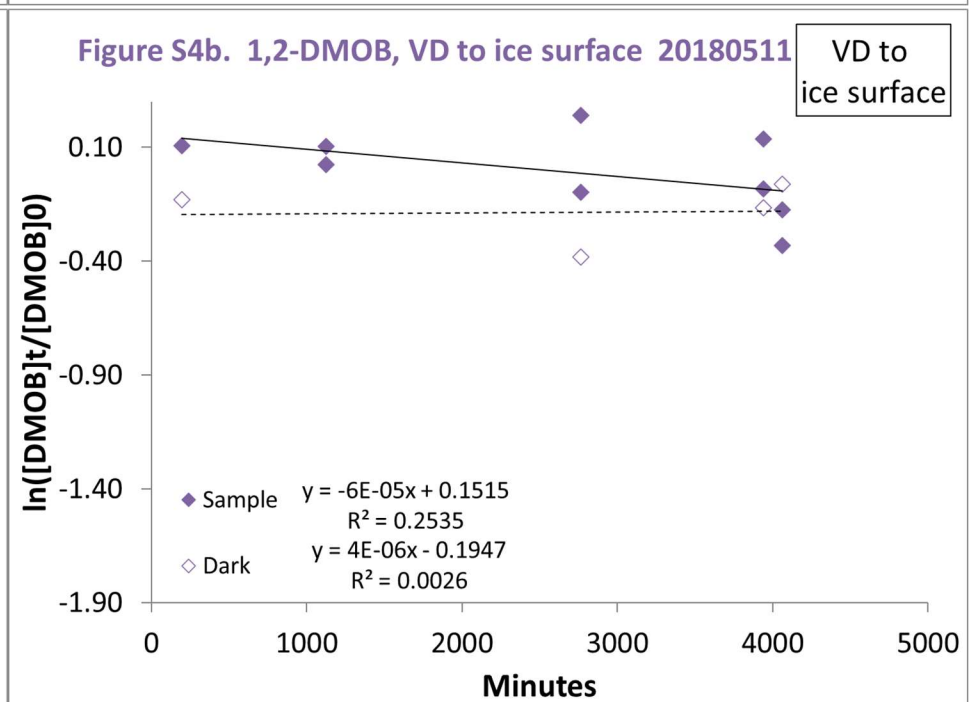
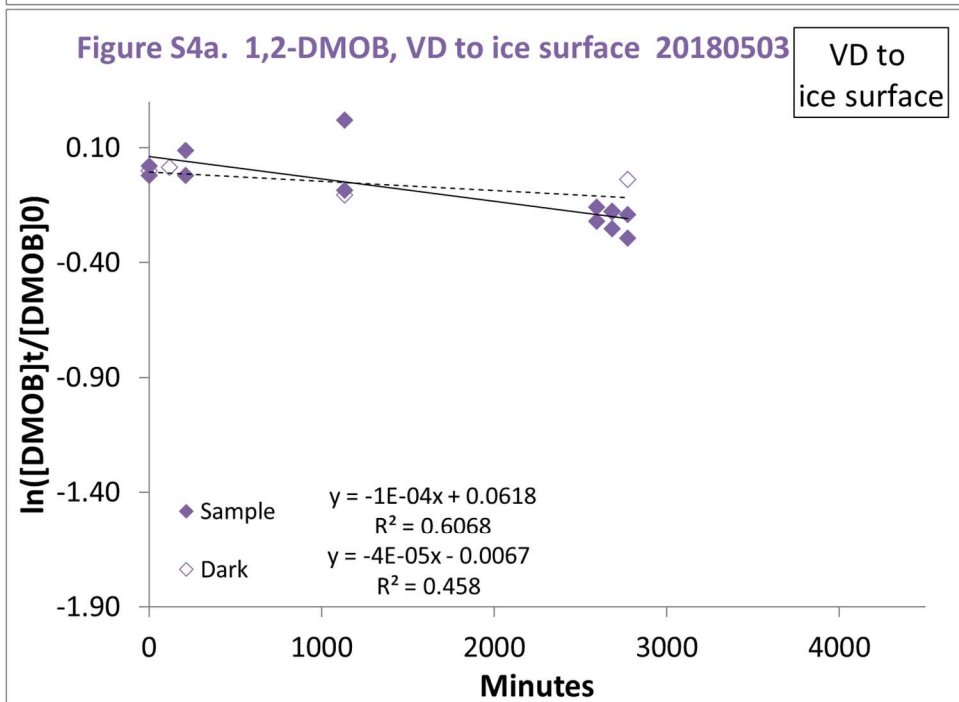
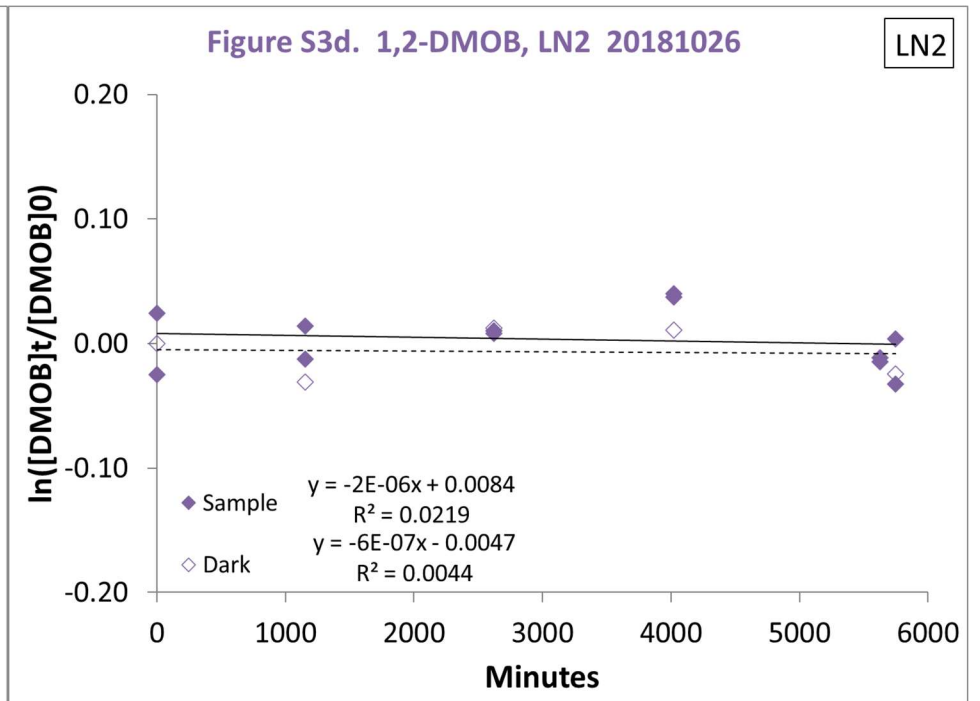
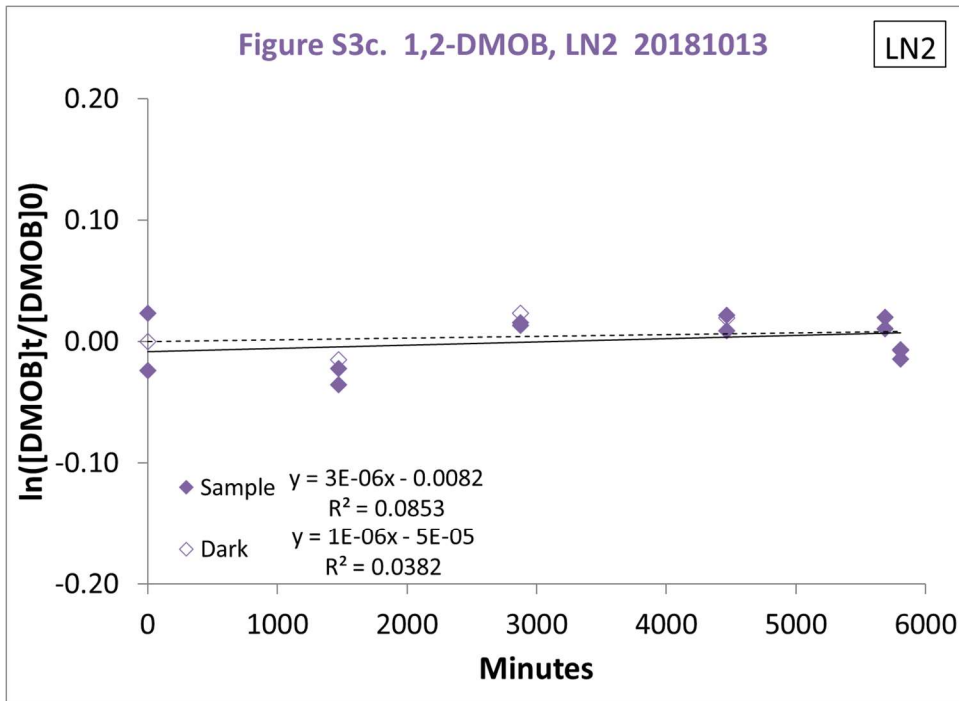
^a Calculated using $\Sigma (2303/N_A I_\lambda \epsilon_\lambda)$, where 2303 is a factor for units and base conversion (1000 cm³ L⁻¹), N_A is Avogadro's number (6.022 × 10²³ molecules mol⁻¹), I_λ is the experimental or modeled photon flux at each wavelength (photons cm⁻² s⁻¹ nm⁻¹), and ϵ_λ is the wavelength-dependent molar absorptivity for each DMOB (M⁻¹ cm⁻¹).

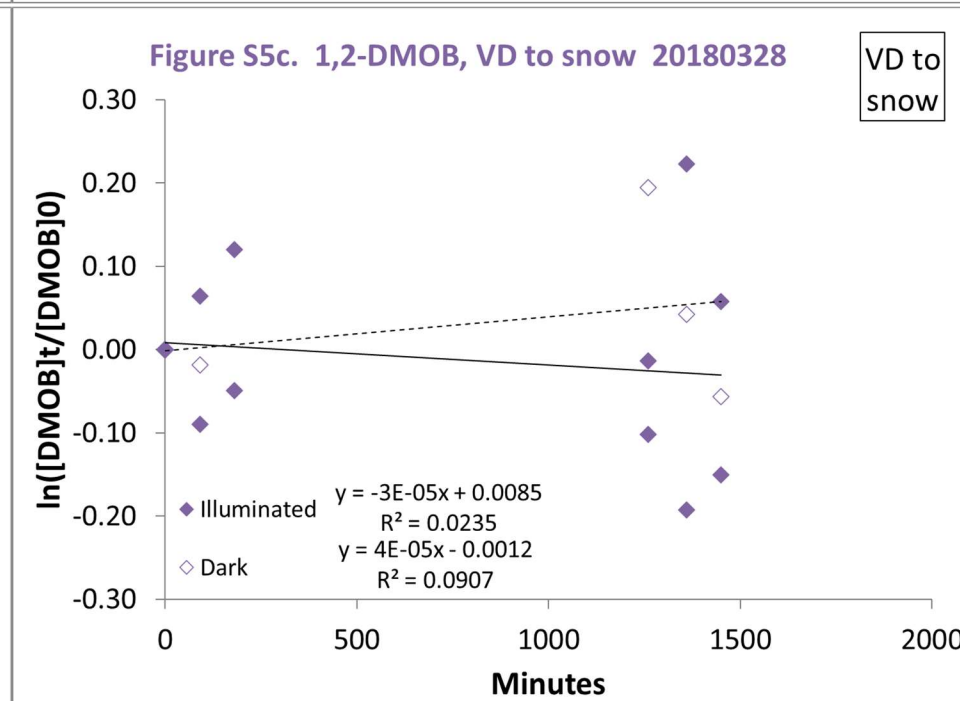
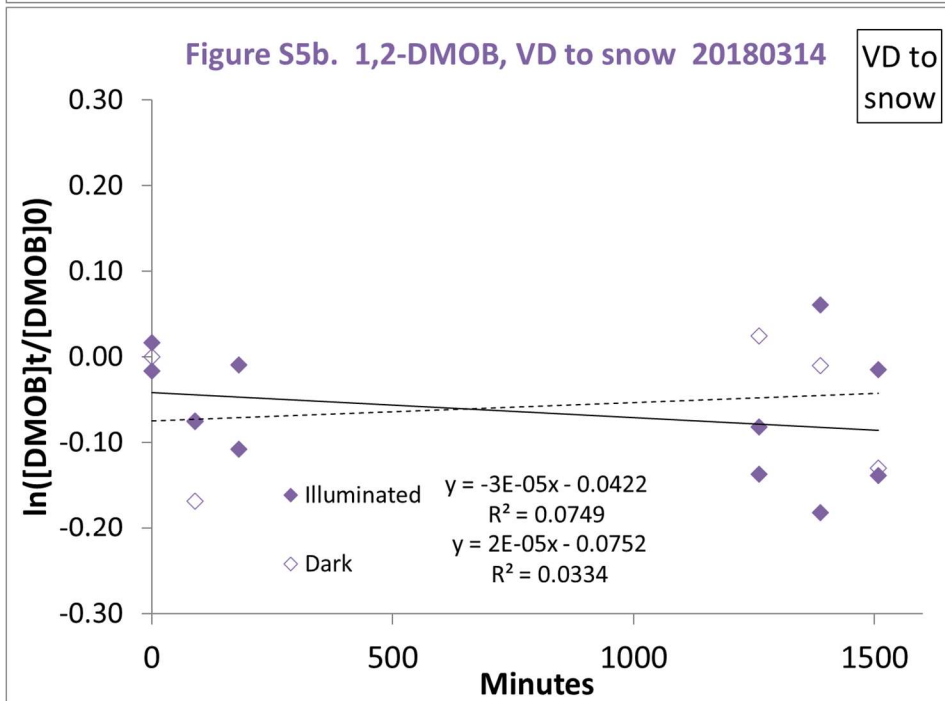
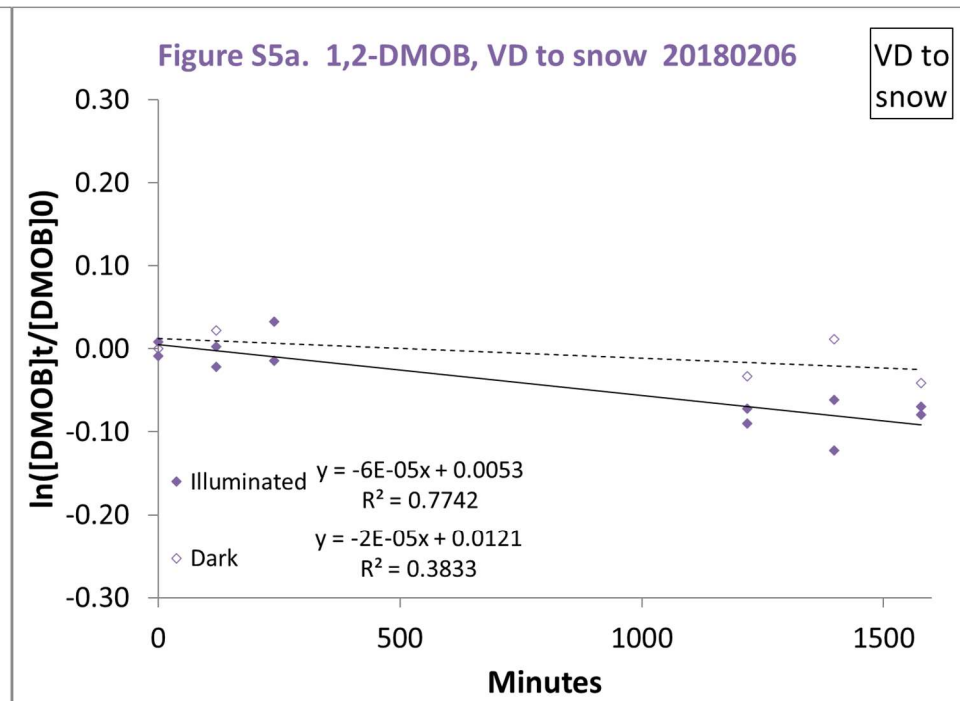
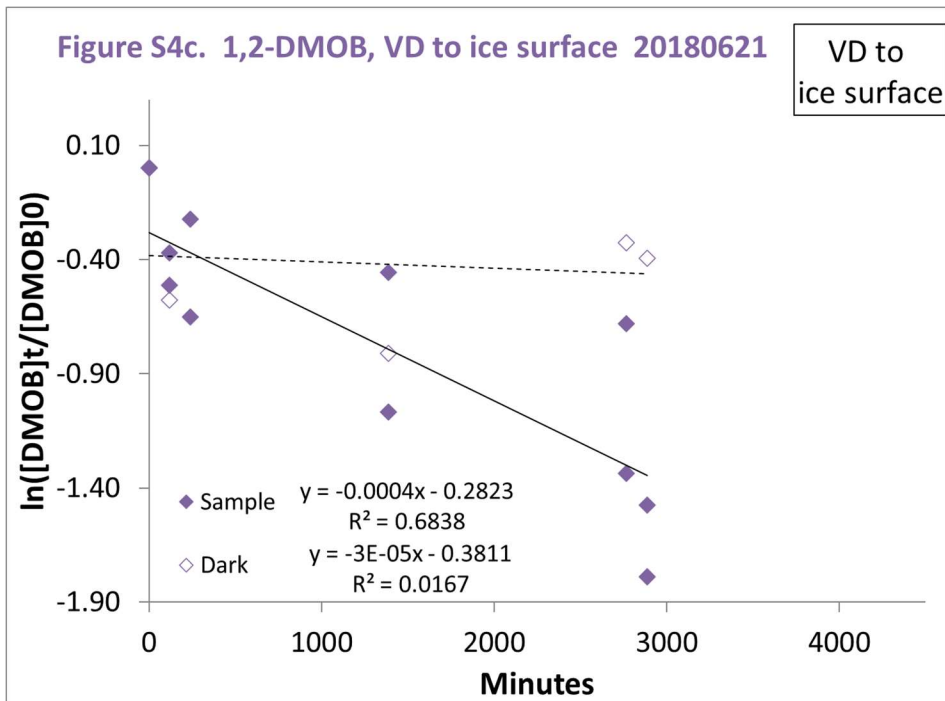
Supplemental Table S5. Machine learning training and testing errors. Summary of training and testing Mean Absolute Error (MAE) for each DMOB molecule in the machine learning model of light absorption. Both the training and the testing MAE are computed by averaging the MAE from the 5-fold cross validation scheme.

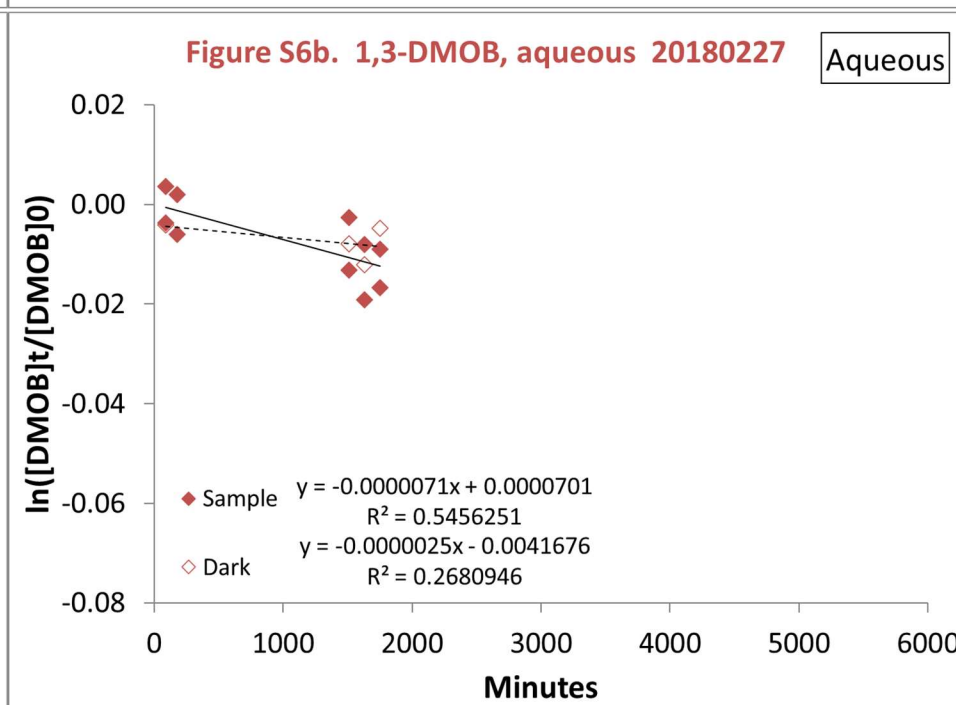
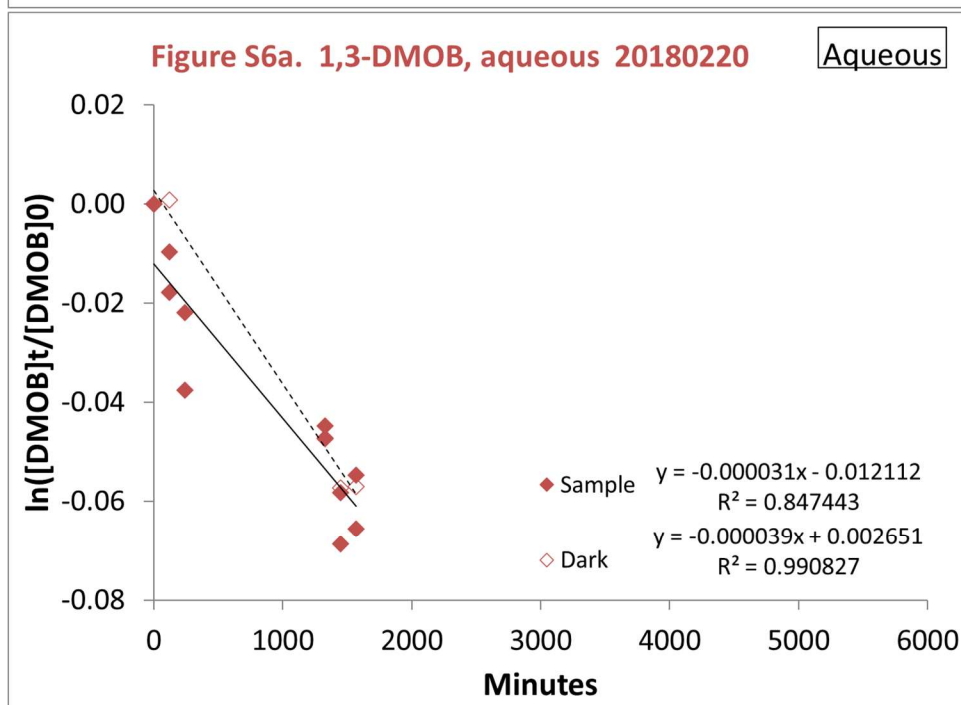
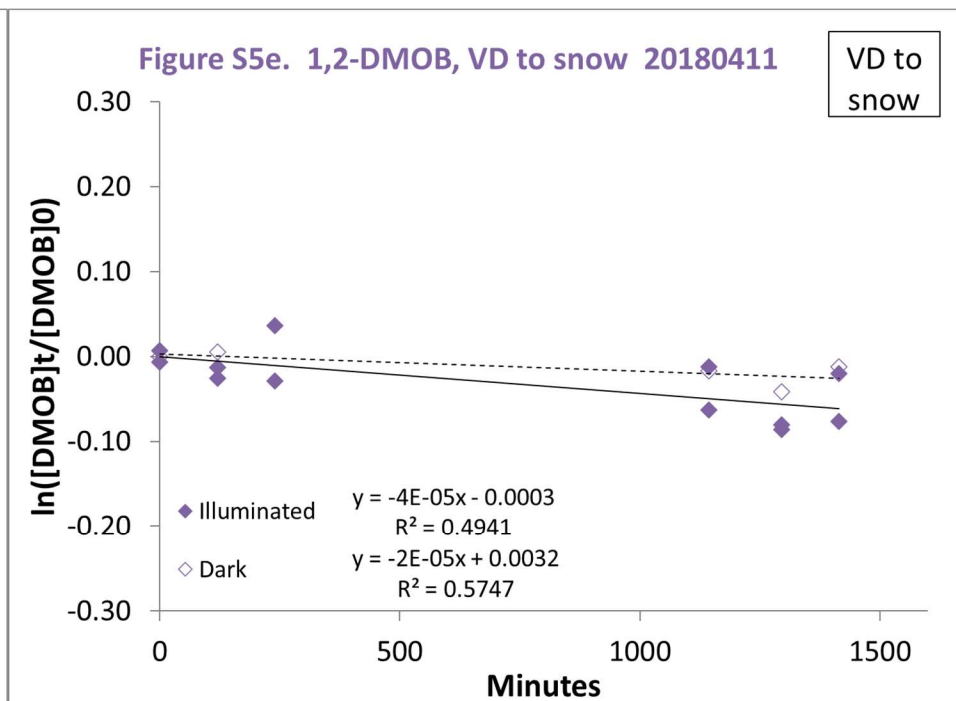
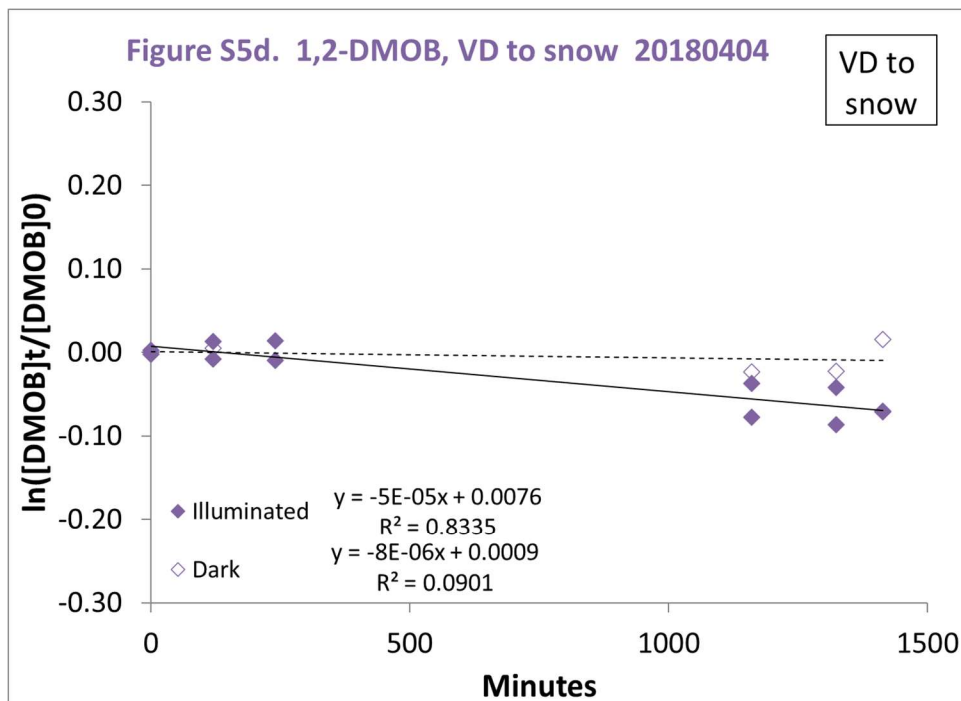
Summary of mean absolute error (MAE) from the ML model		
	Training MAE (nm)	Testing MAE (nm)
1,2-DMOB	1.38	1.84
1,3-DMOB	1.39	1.92
1,4-DMOB	1.50	1.87
Average & Std	1.42 ± 0.056	1.88 ± 0.031

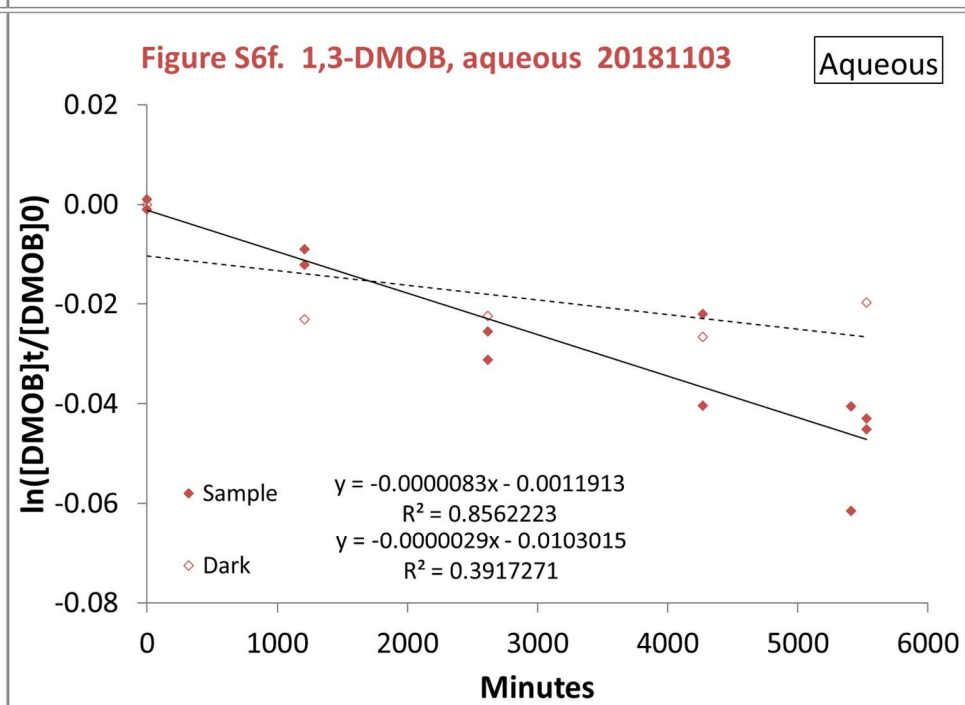
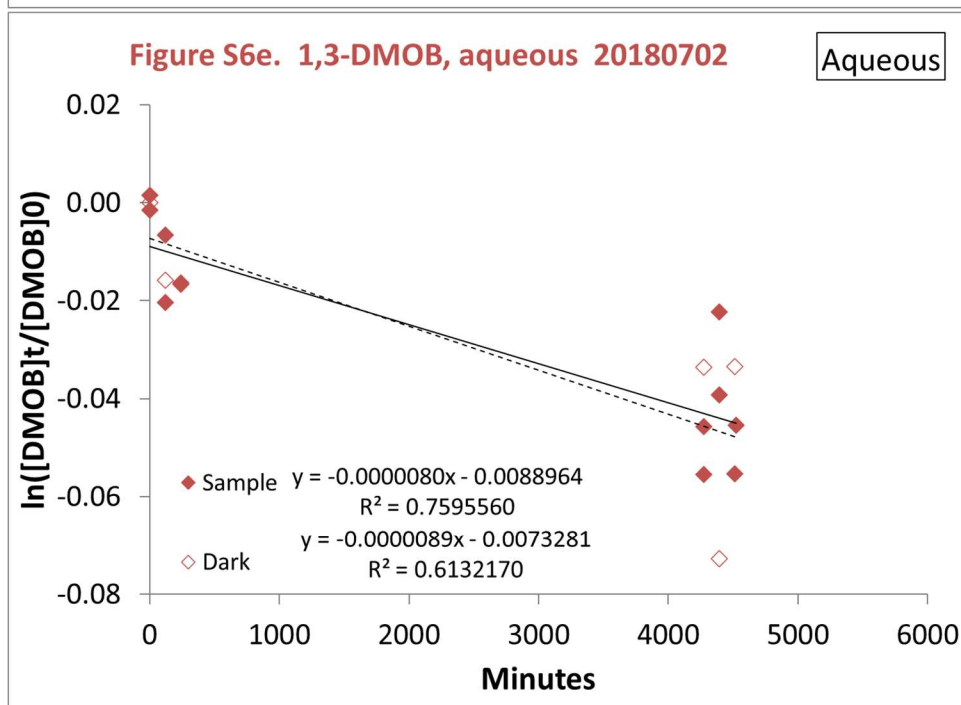
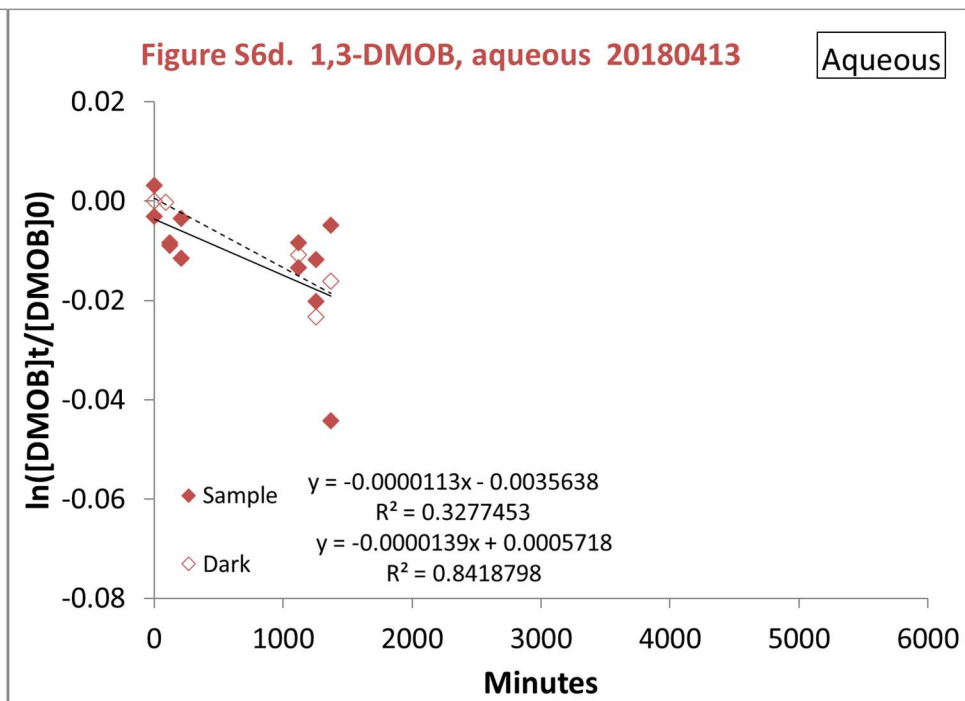
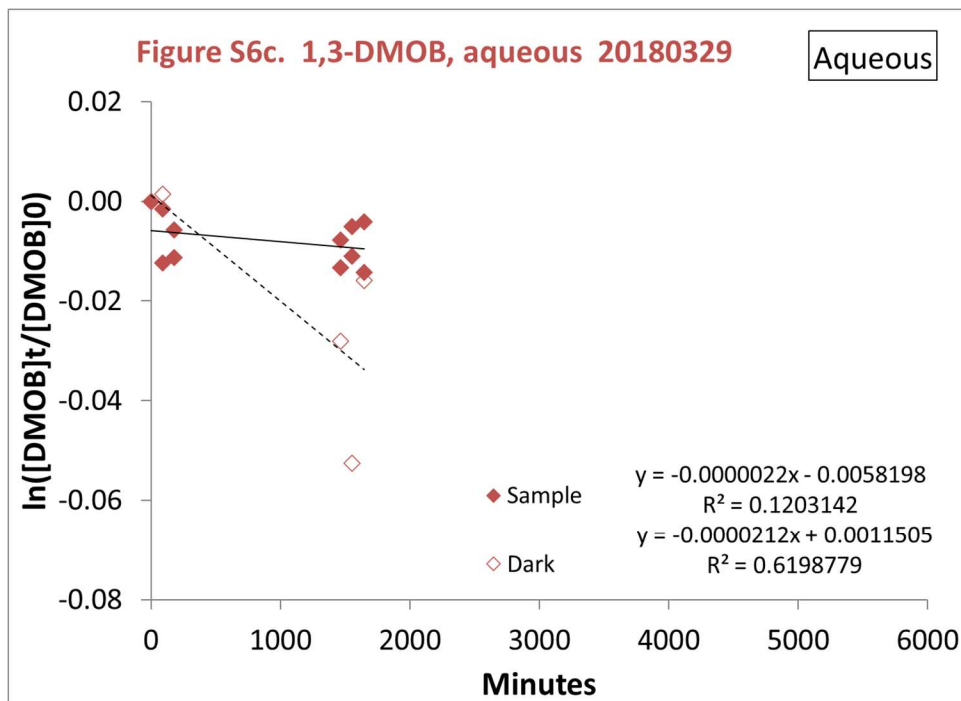


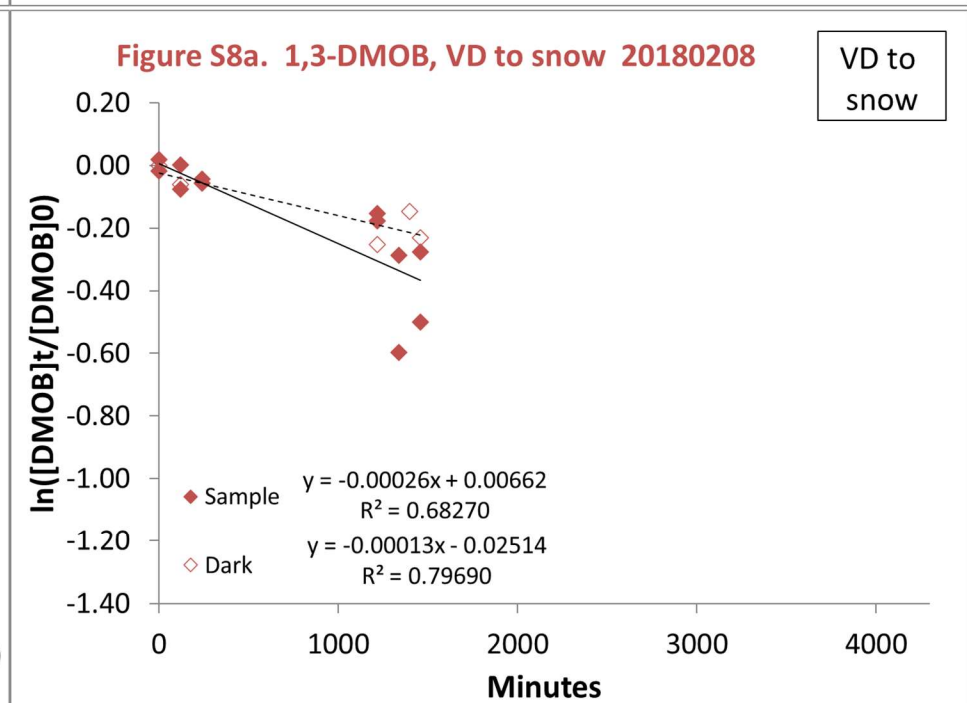
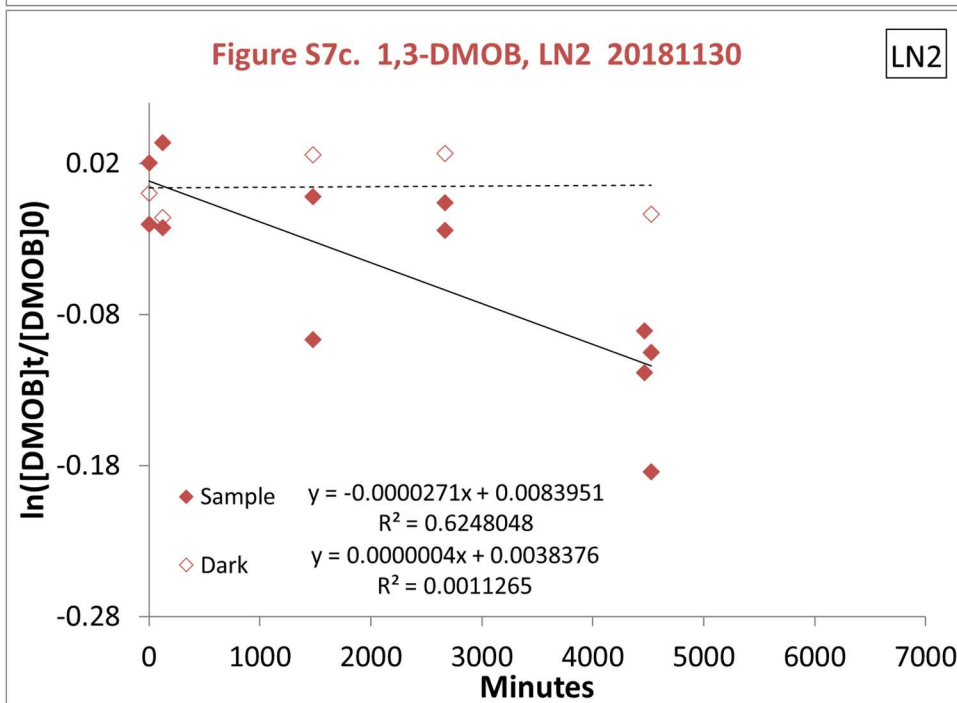
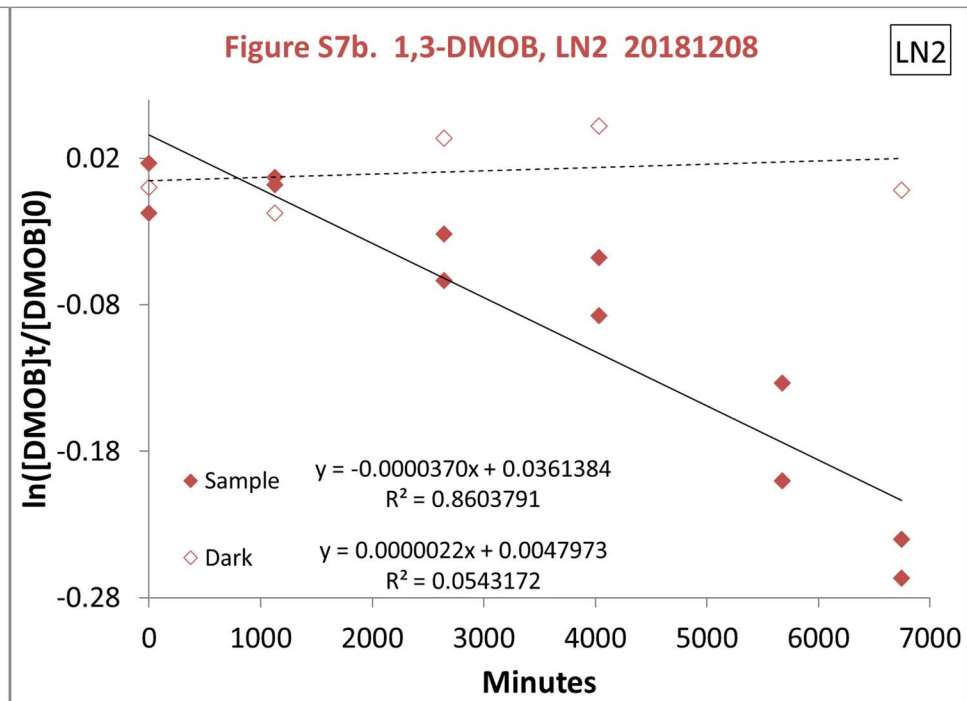
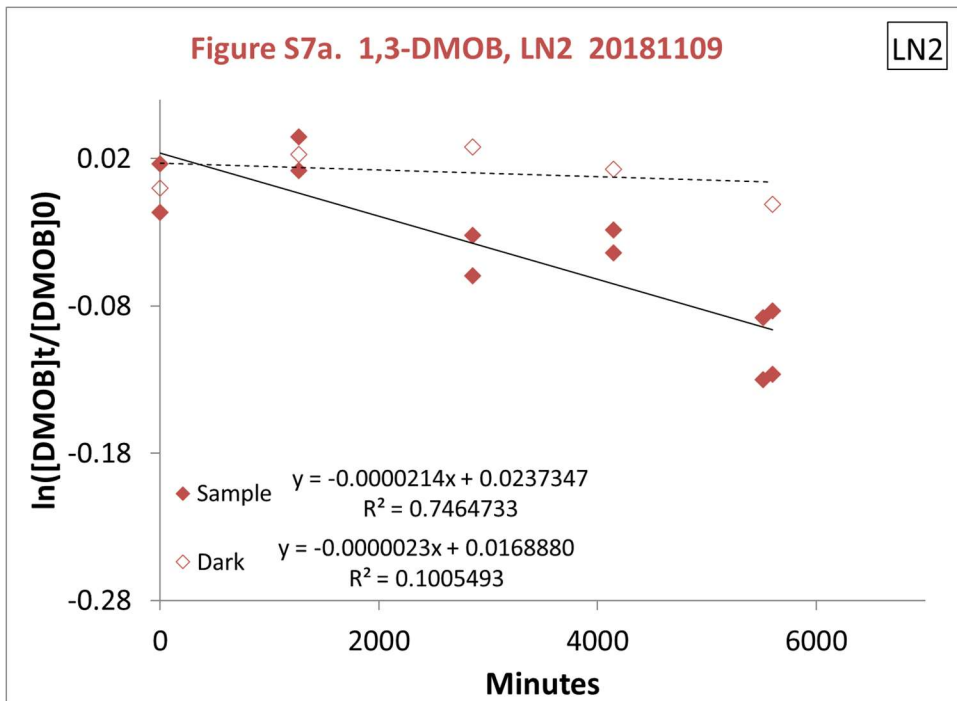


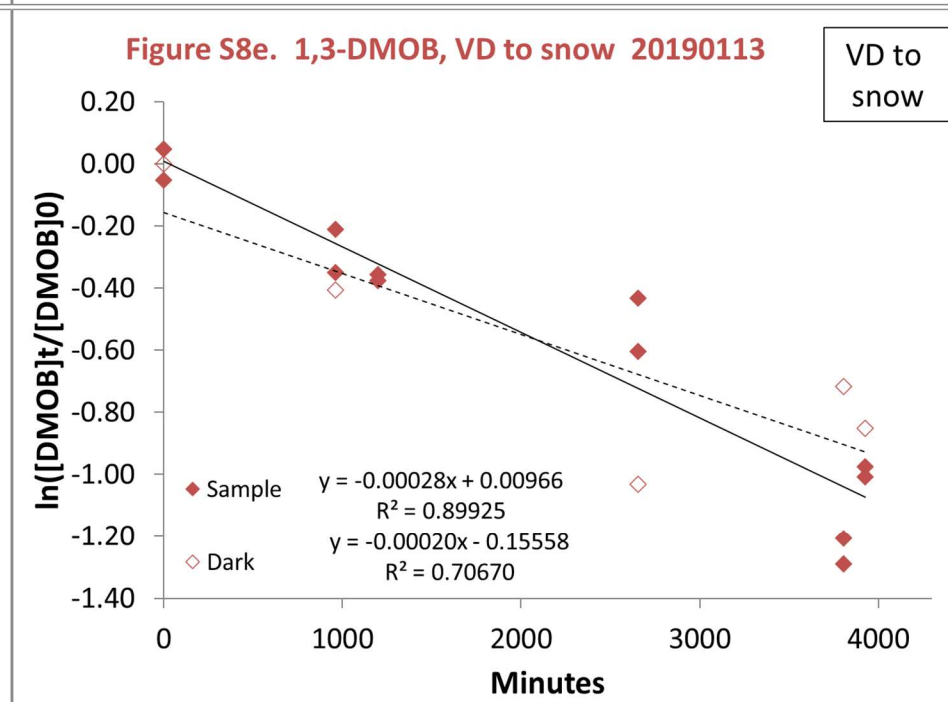
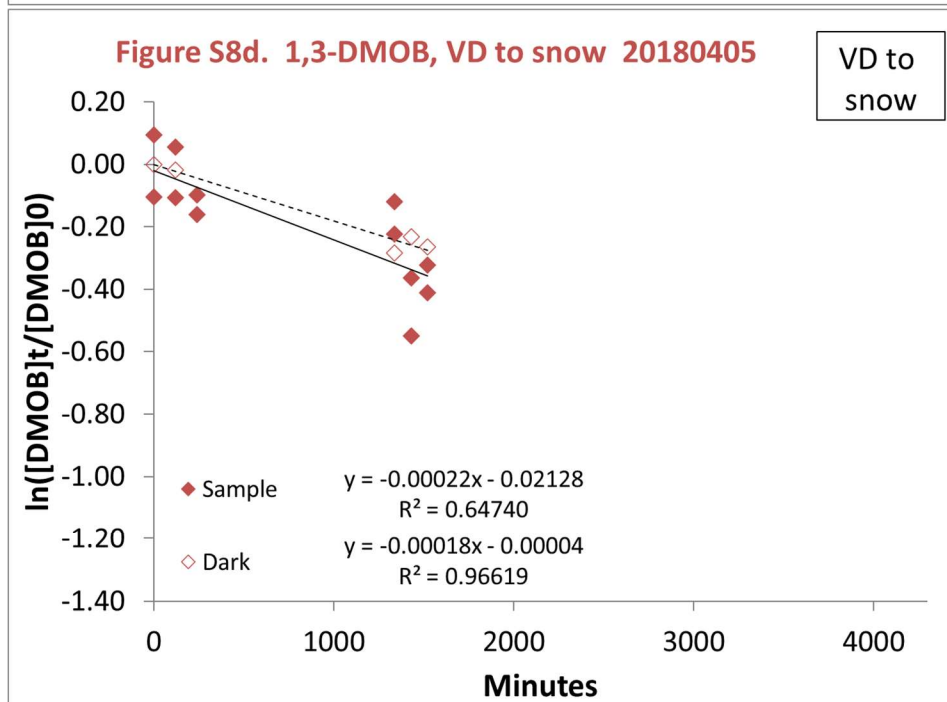
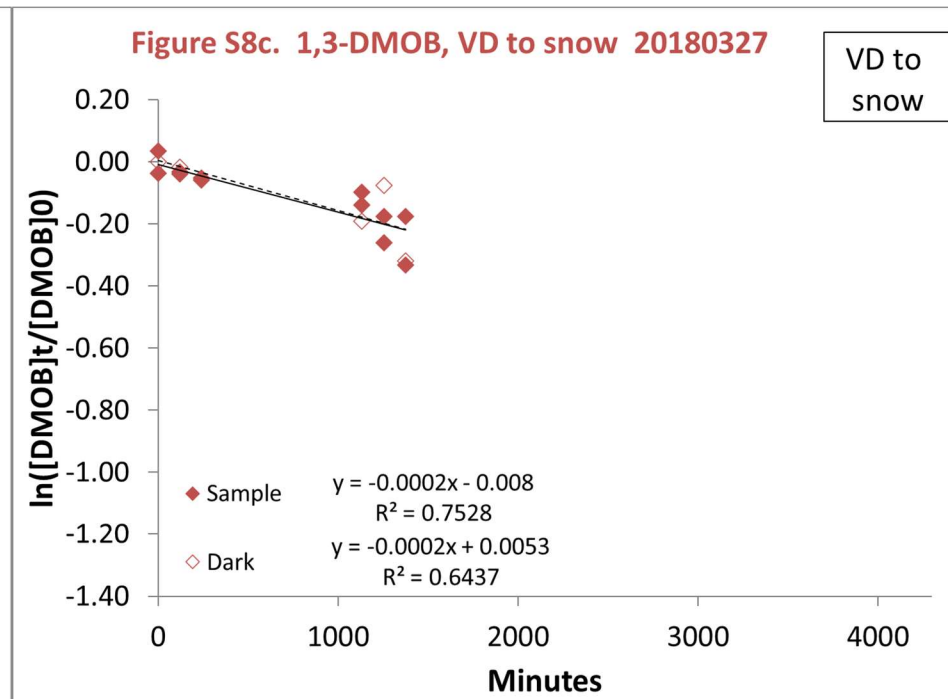
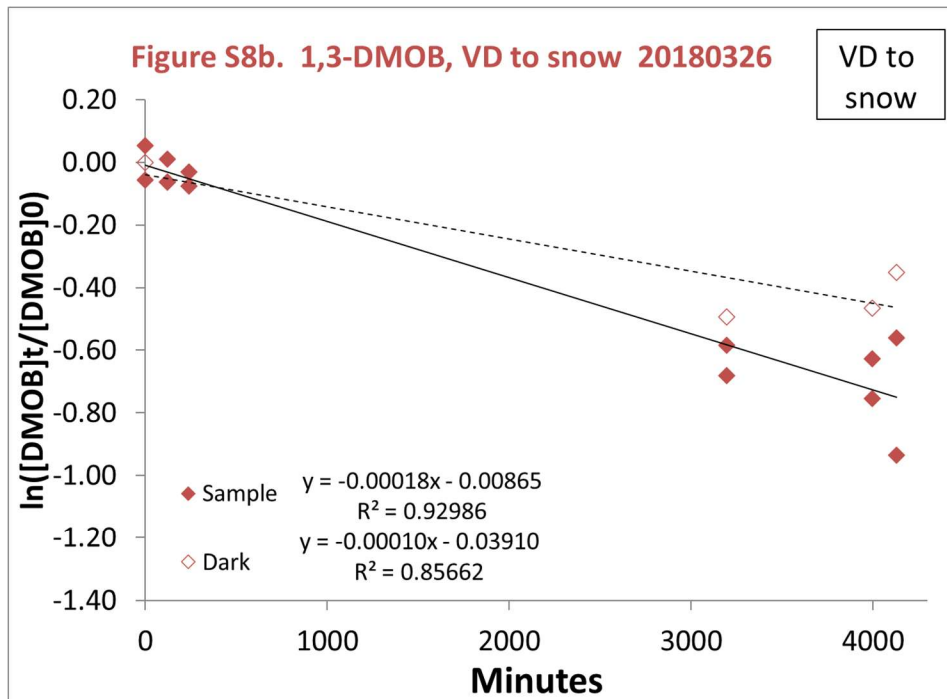


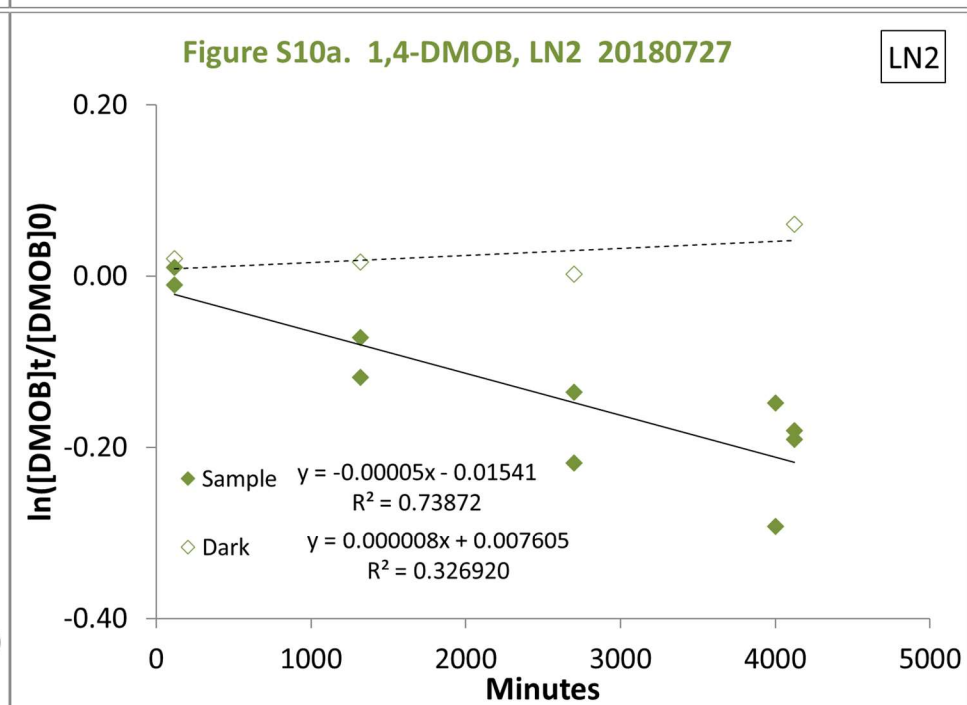
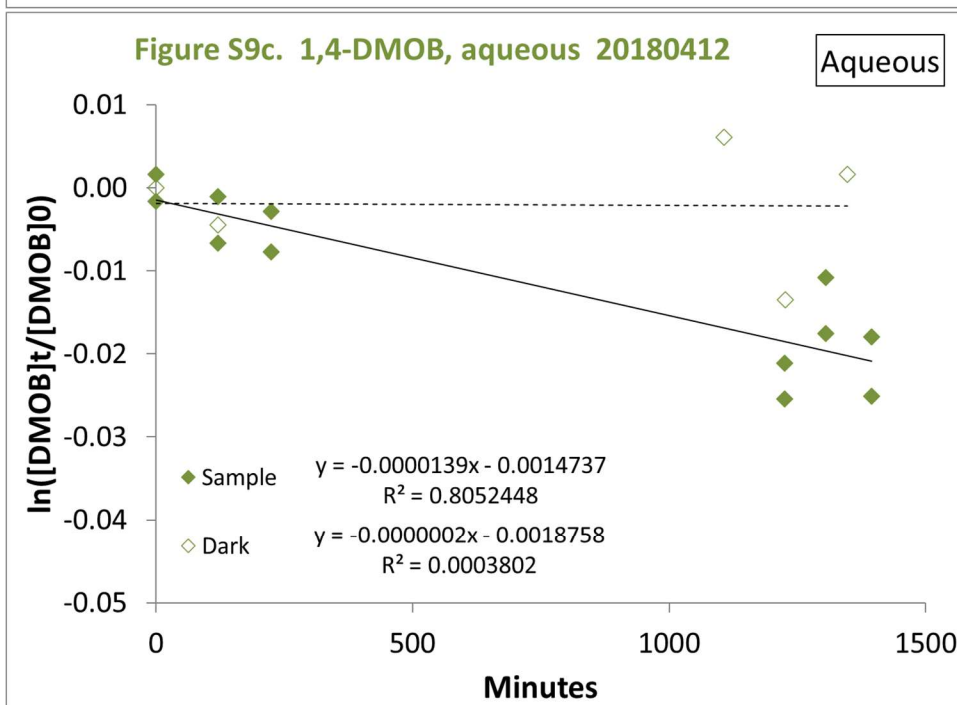
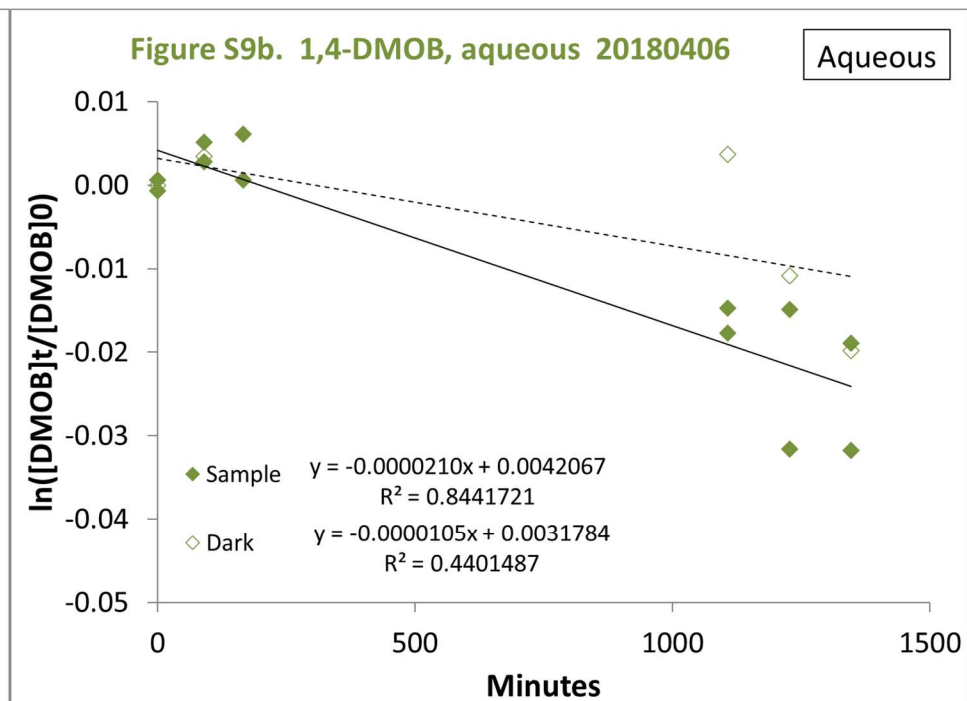
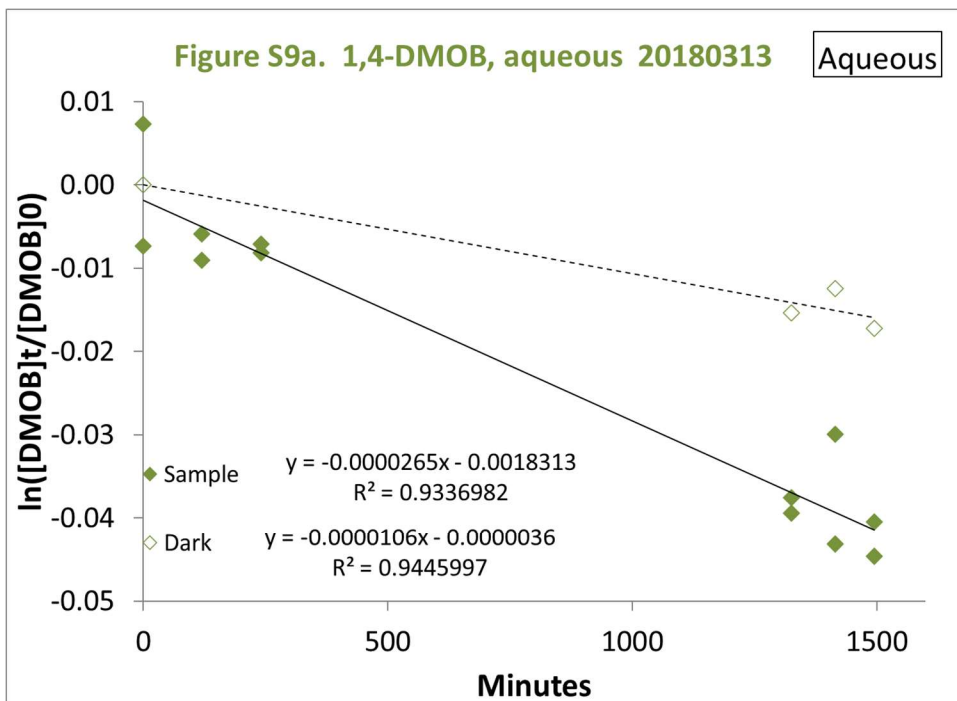


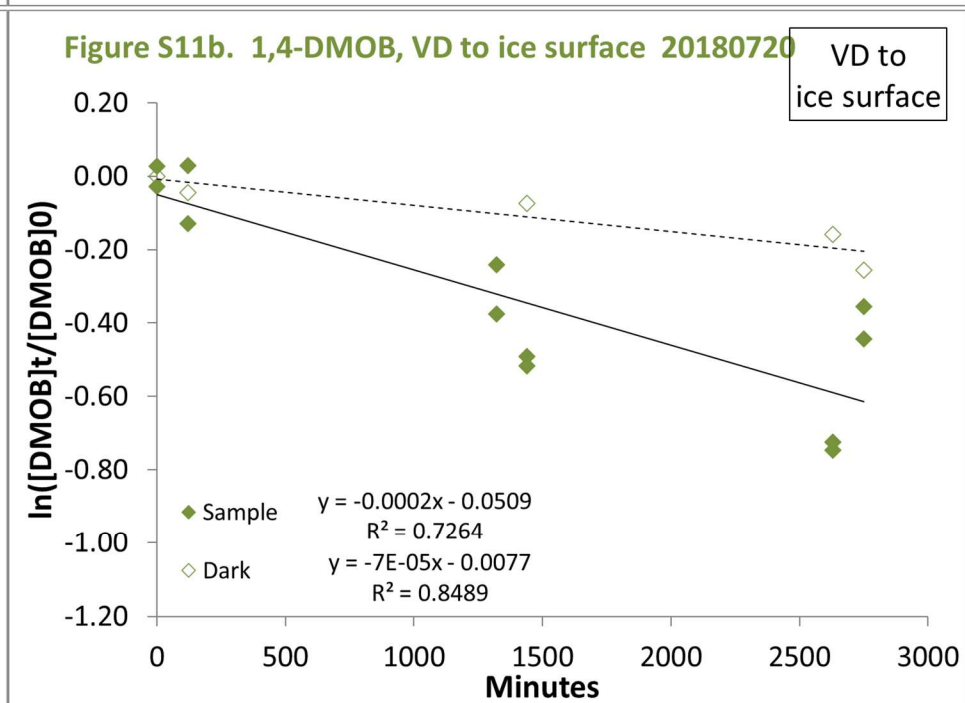
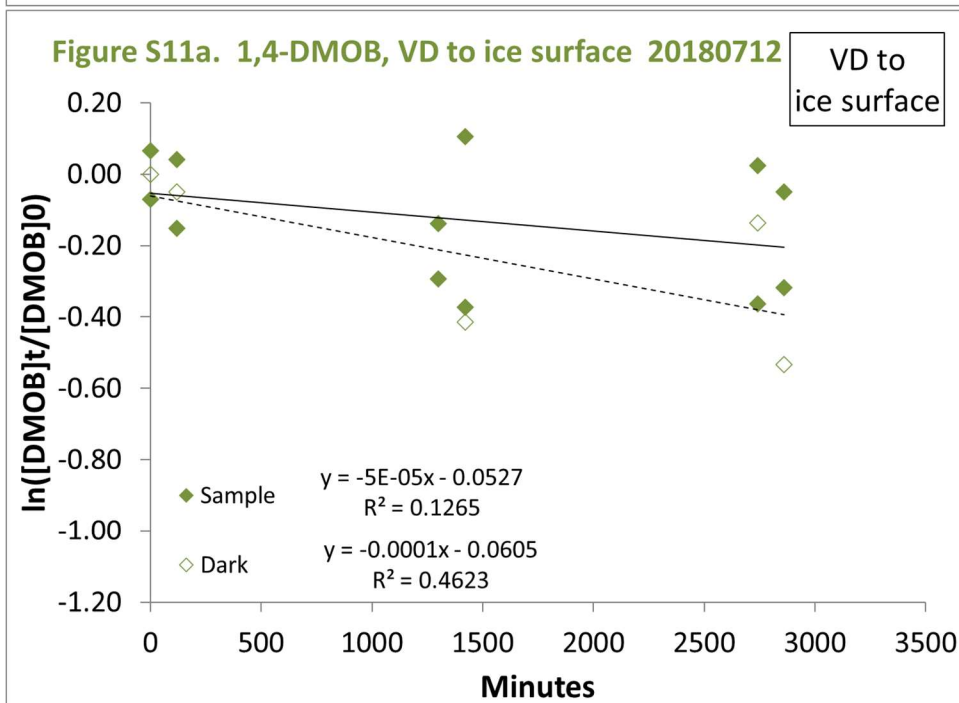
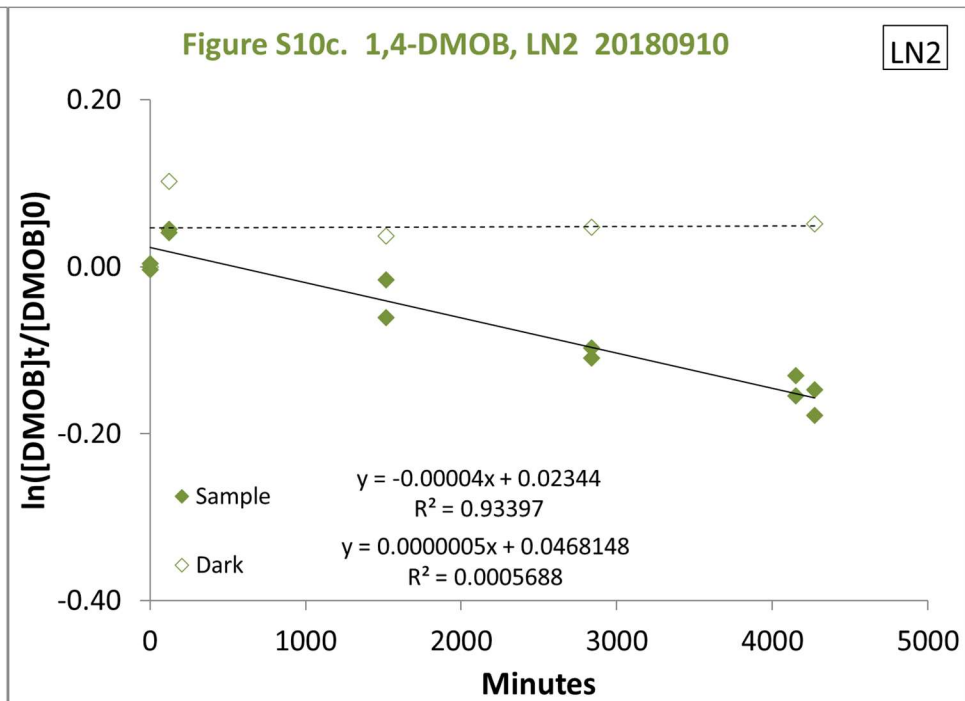
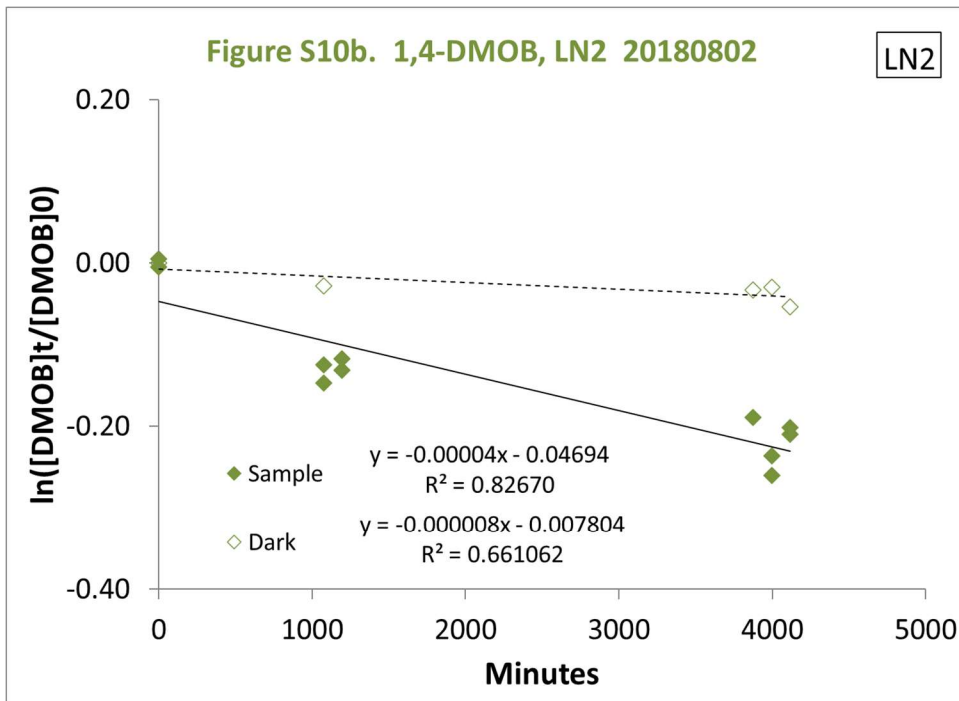


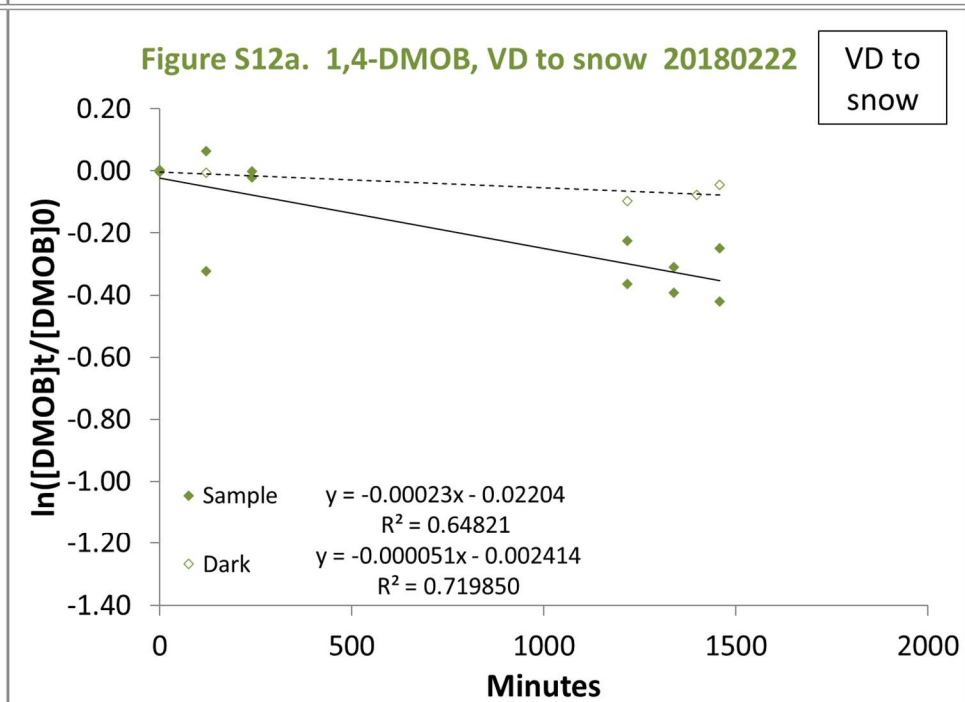
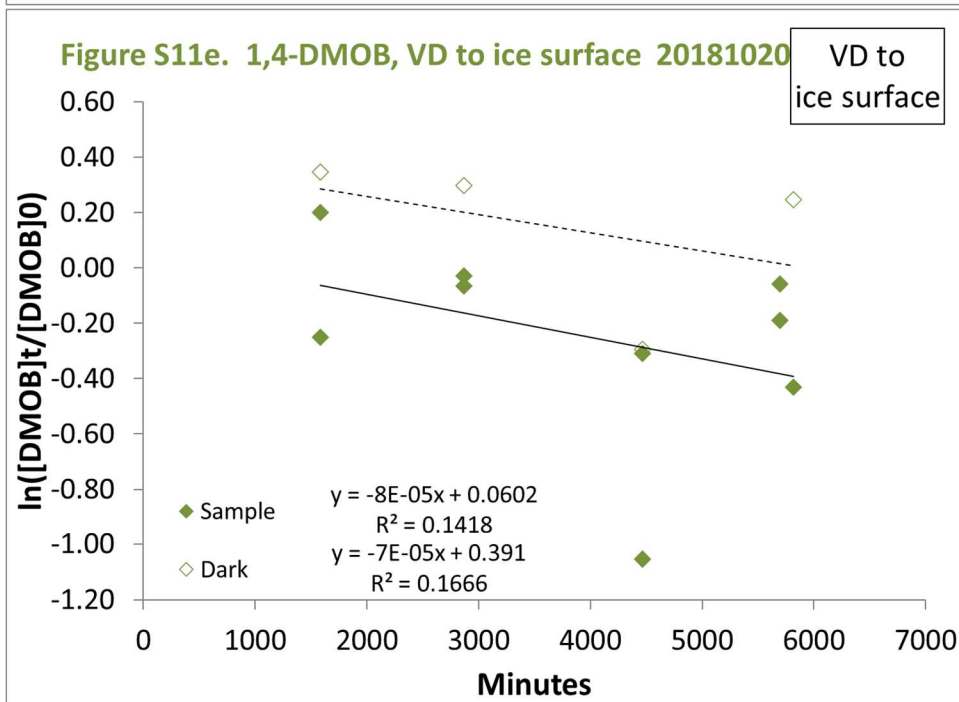
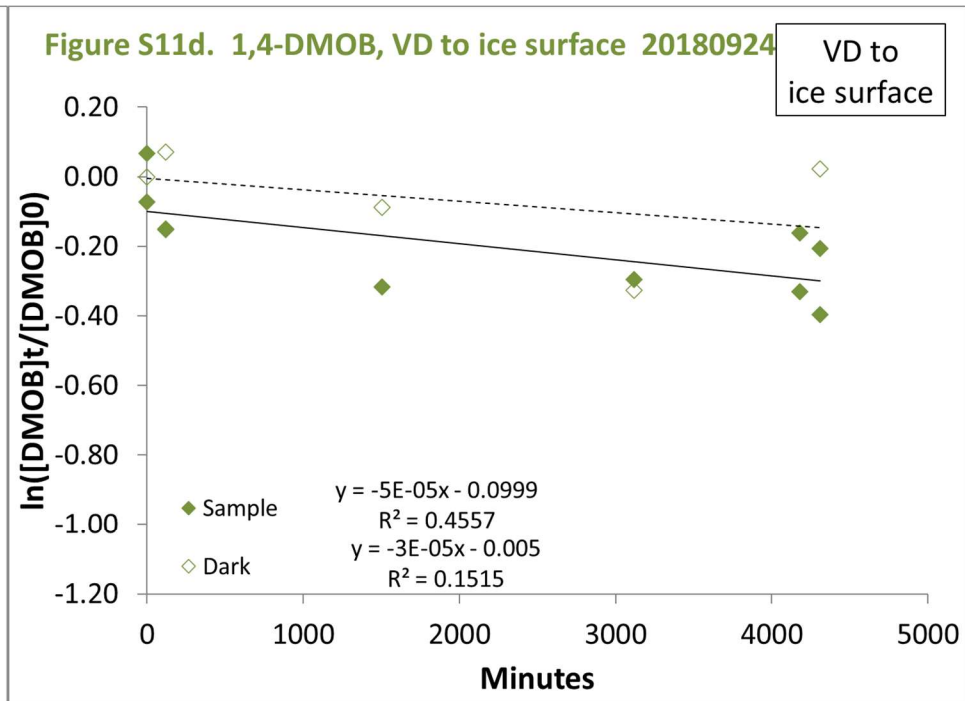
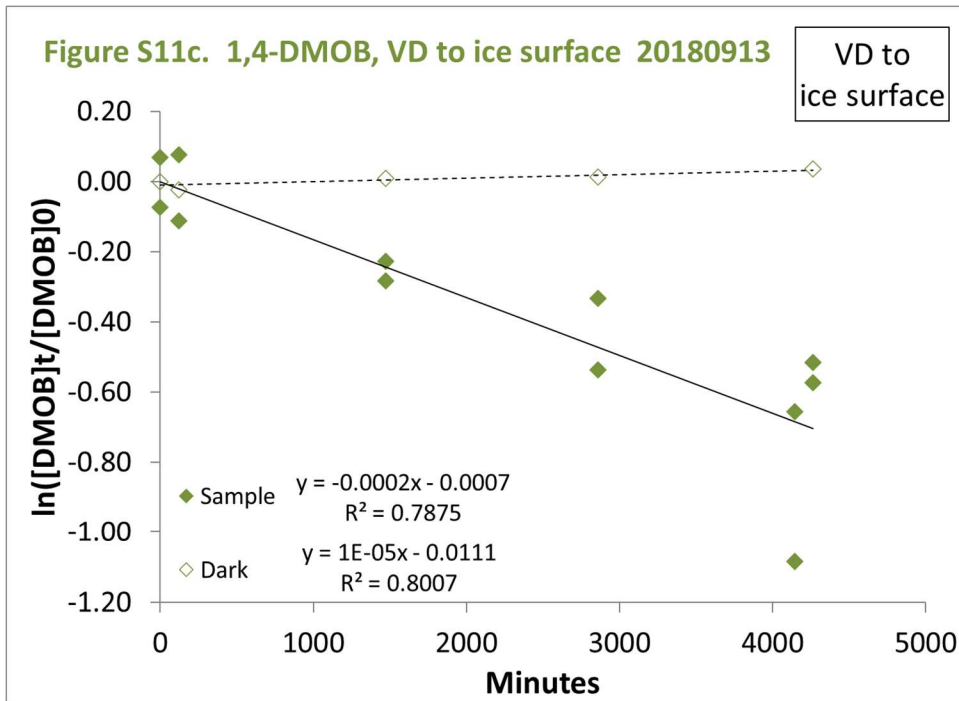


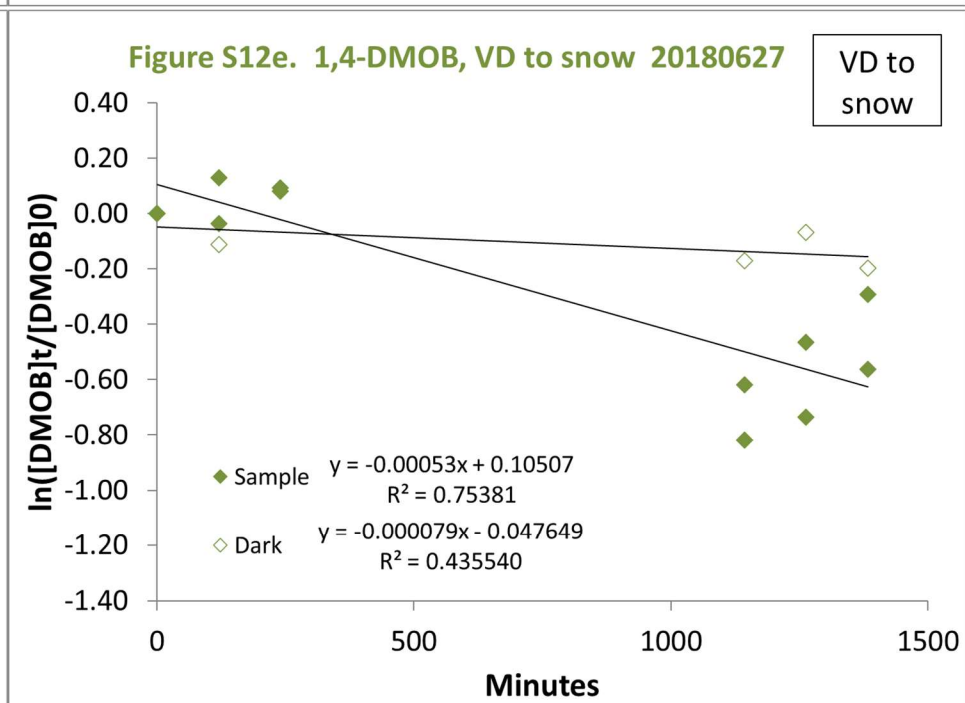
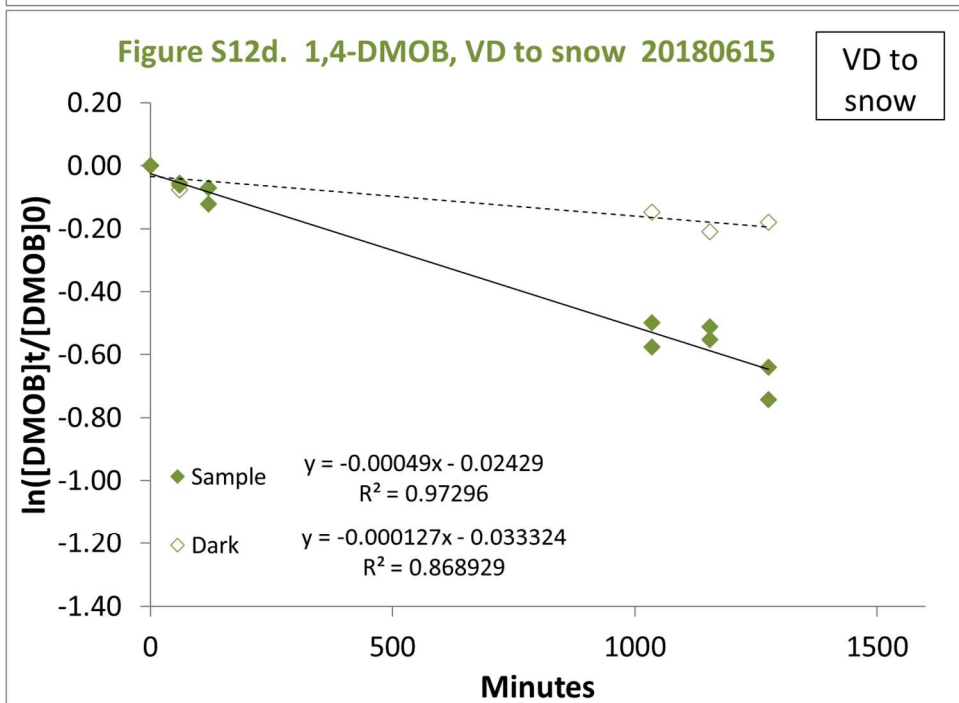
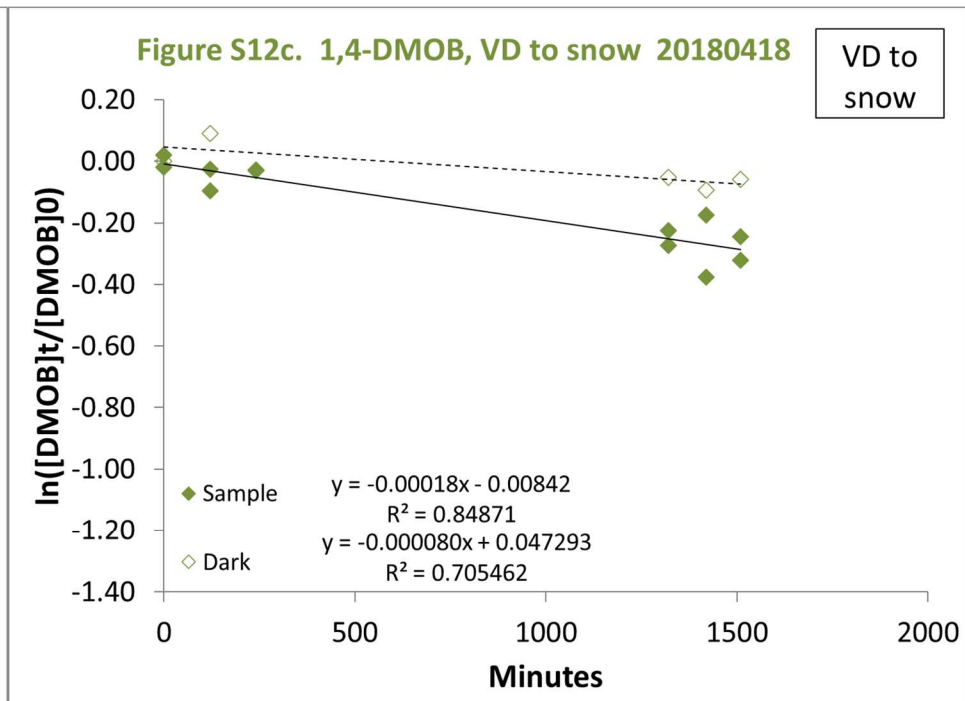
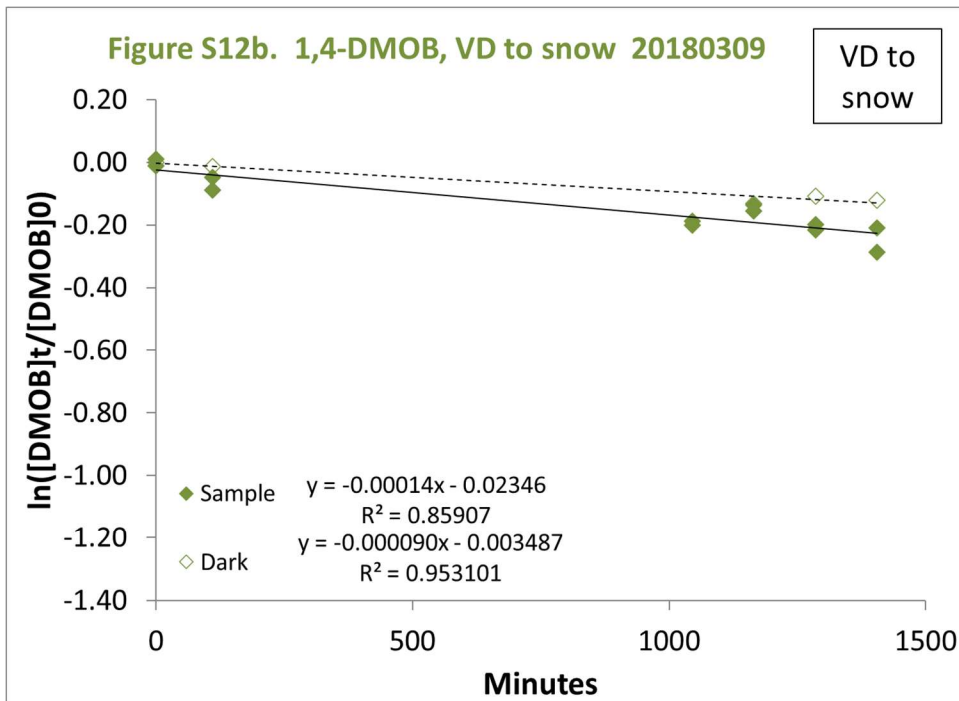


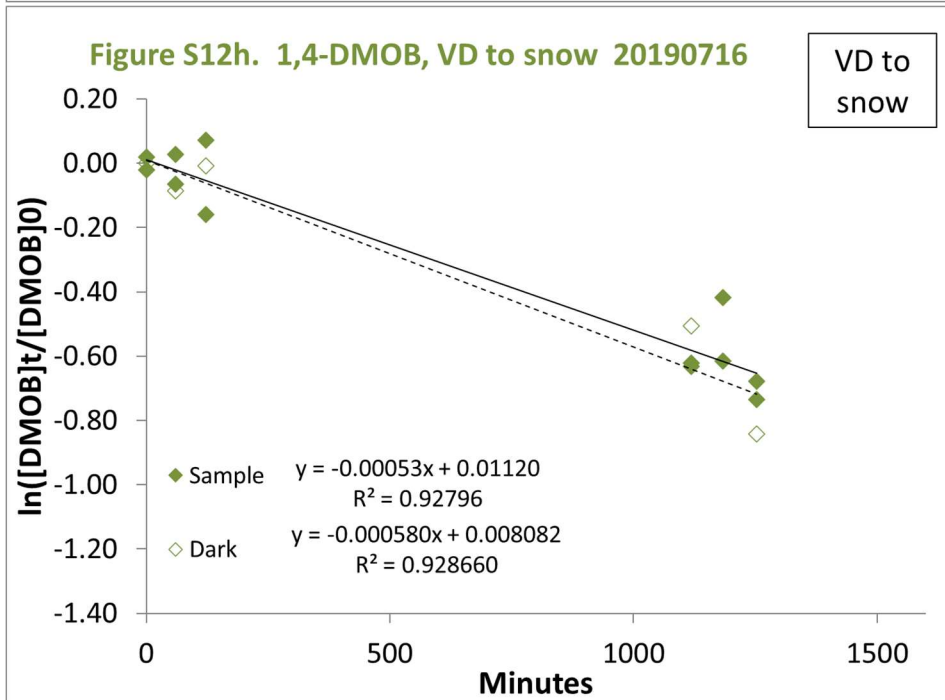
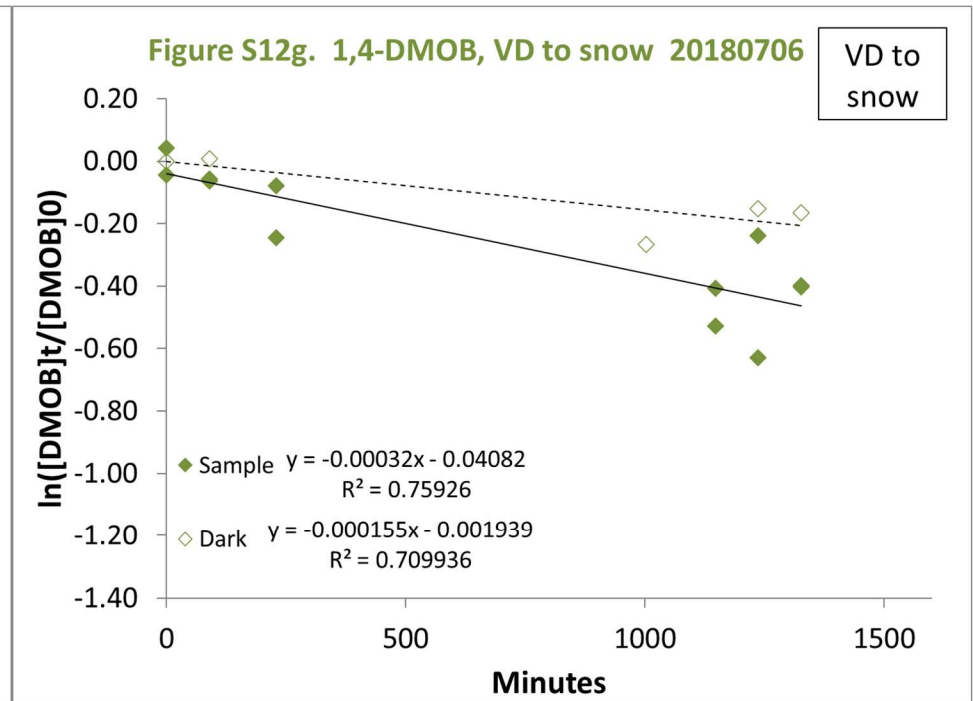
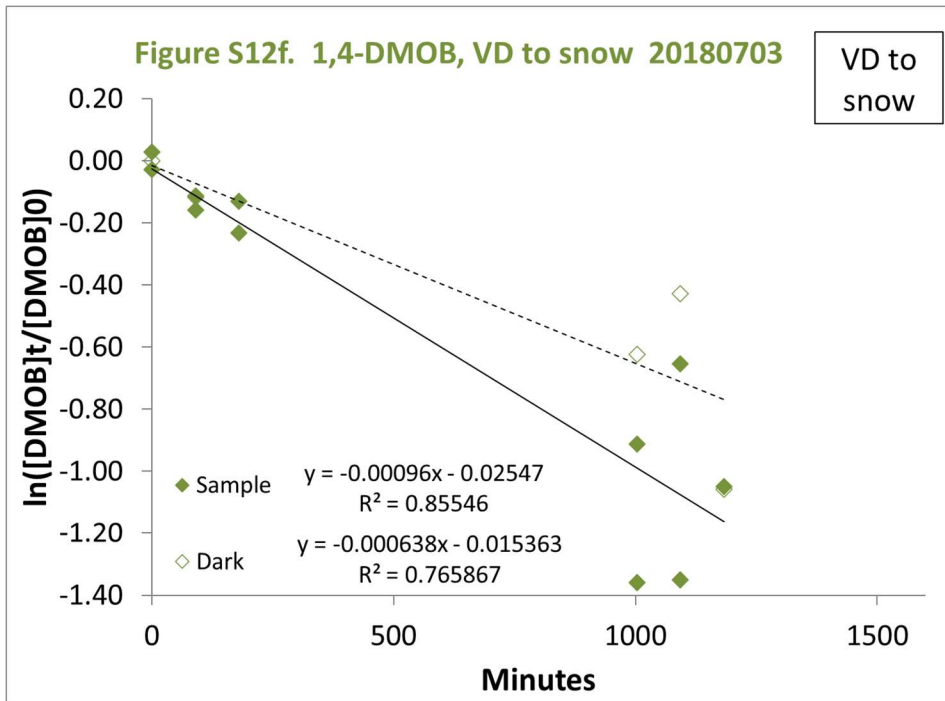




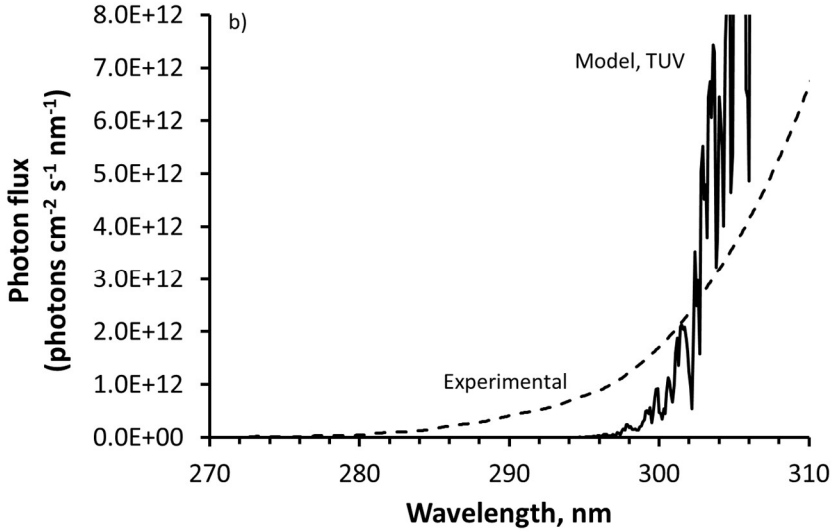
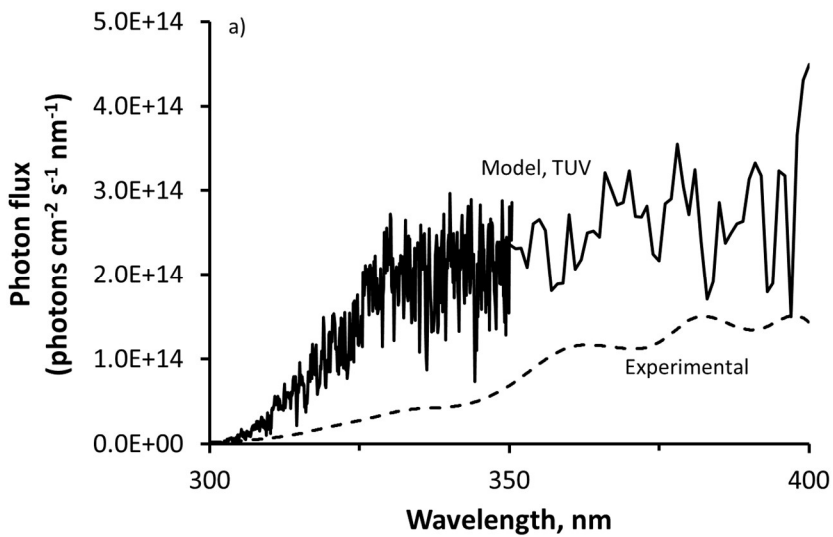




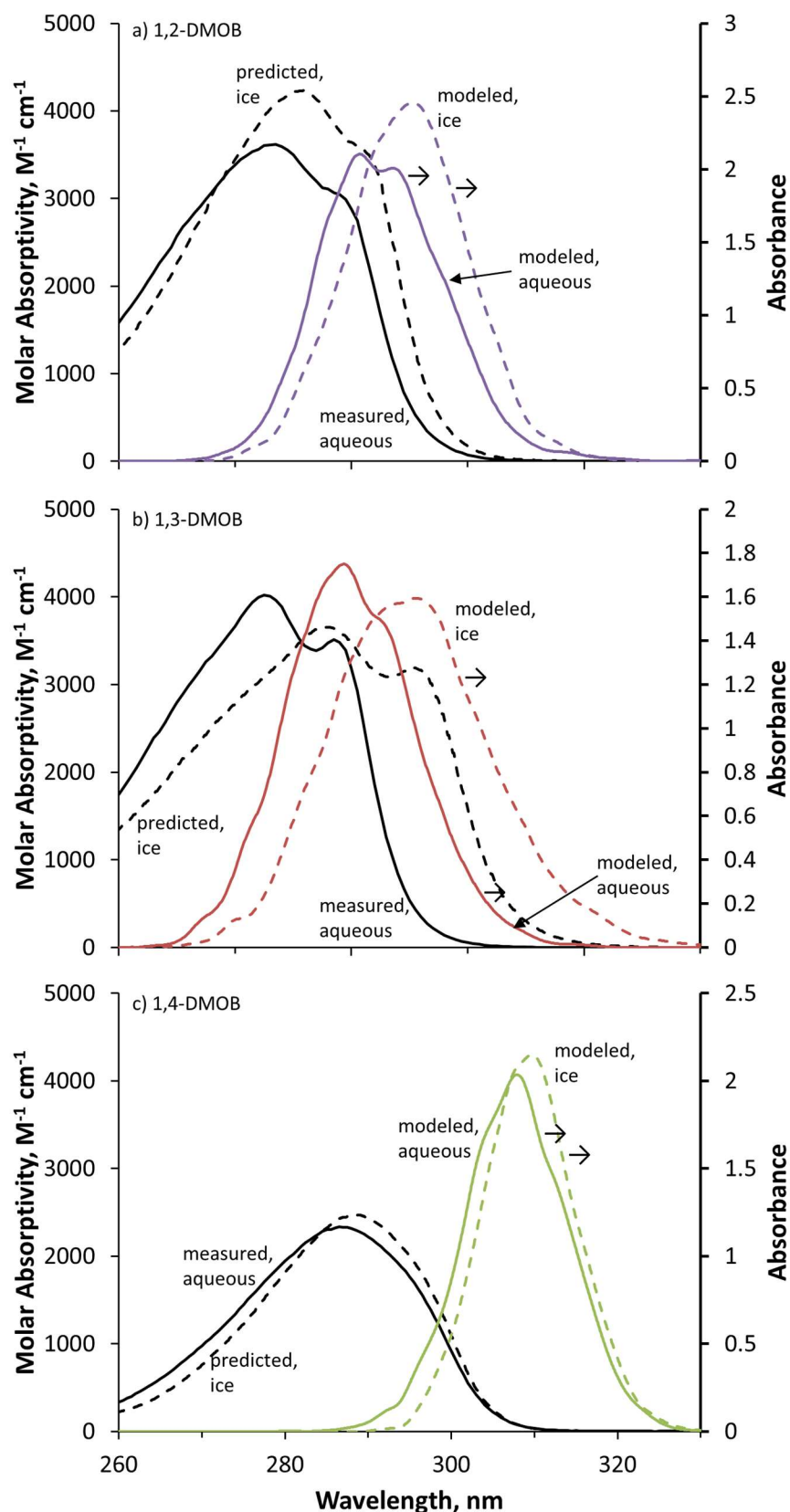




Supplemental Figures S1a-S12h. Results for individual illumination experiments. Results for individual illumination experiments showing dimethoxybenzene concentration changes over time for illuminated samples (filled diamonds, solid regression line) and dark controls (open diamonds, dashed regression line). Date for each experiment is given in yyymmdd format. Compounds are color-coded purple (1,2-DMOB), maroon (1,3-DMOB), and green (1,4-DMOB). Sample type is given in the upper right corner of each graph. Each data point represents an individual sample beaker, with two illuminated samples and one dark control sample per time point. Wherever possible, for each compound the same Y axis scale was used for related sample treatments to allow easier comparison. Average data for each experiment type are summarized in Table S3.

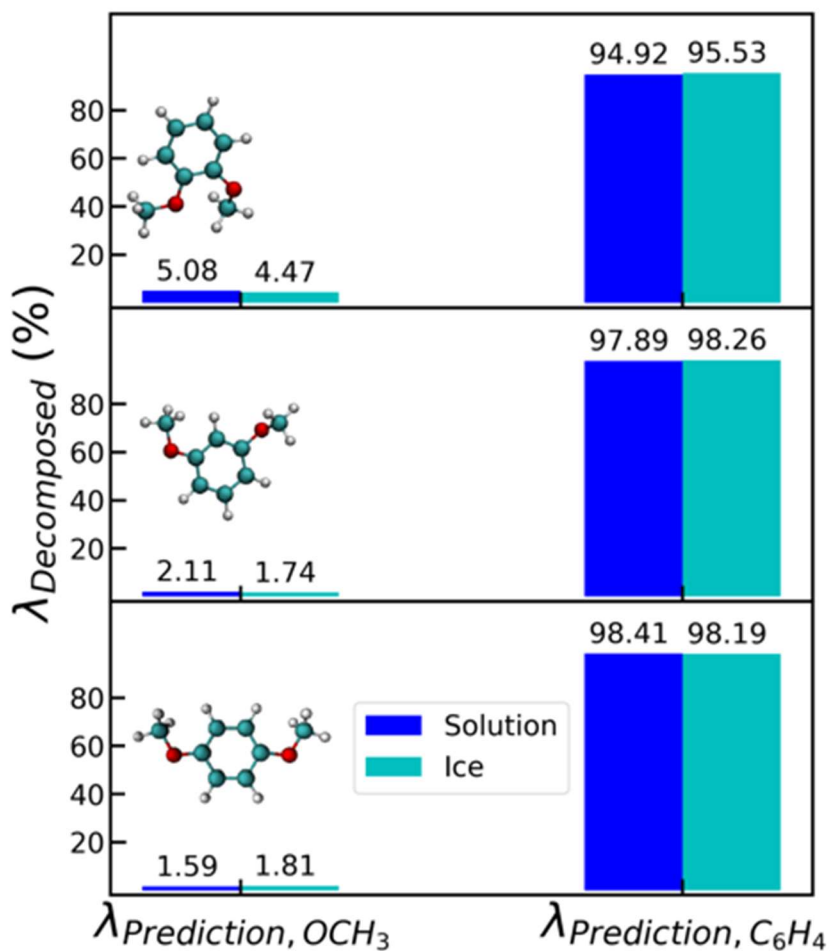


Supplemental Figure S13. Experimental and modeled photon fluxes. Experimental and TUV-modeled photon fluxes from 300-400 nm (panel a) and 270-310 nm (panel b). TUV-modeled flux is for Summit, Greenland at noon on the summer solstice (see text for details of modeling parameters). a) Summit actinic flux is given at 0.1 nm resolution from 300-350 nm, then 1 nm resolution from 350-400 nm; experimental flux was determined at 1 nm and interpolated to 0.1 nm resolution presented here. b) TUV and experimental fluxes at 0.1 nm resolution.

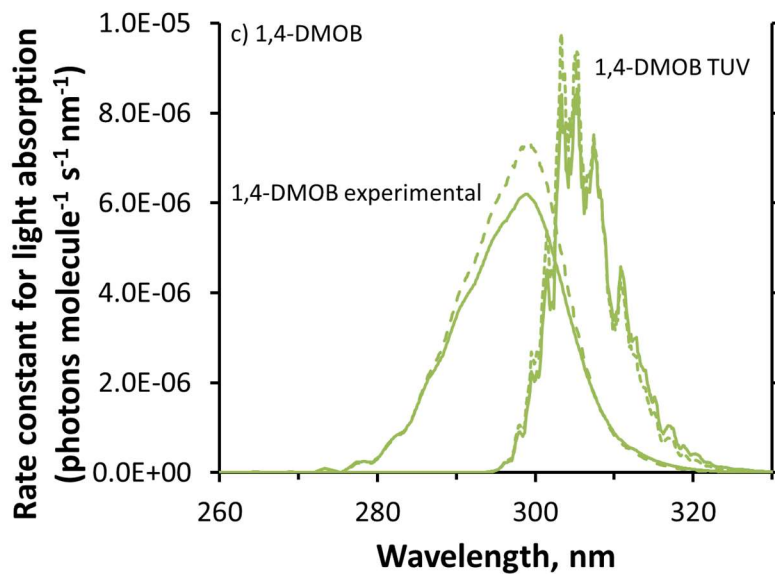
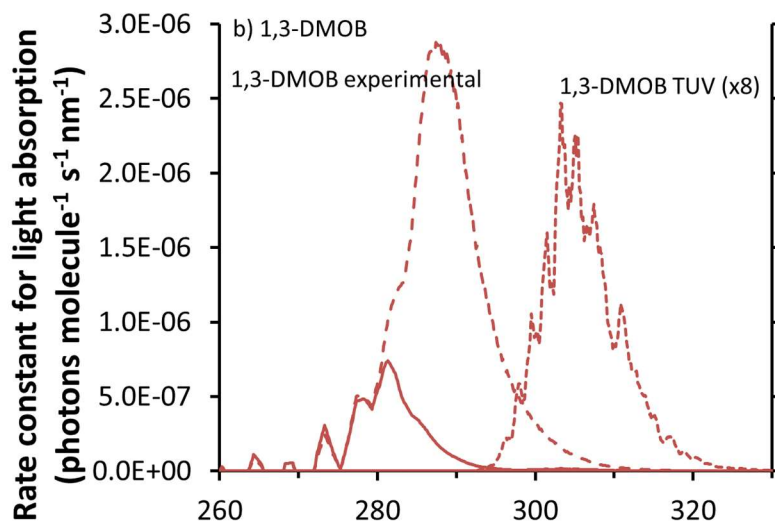
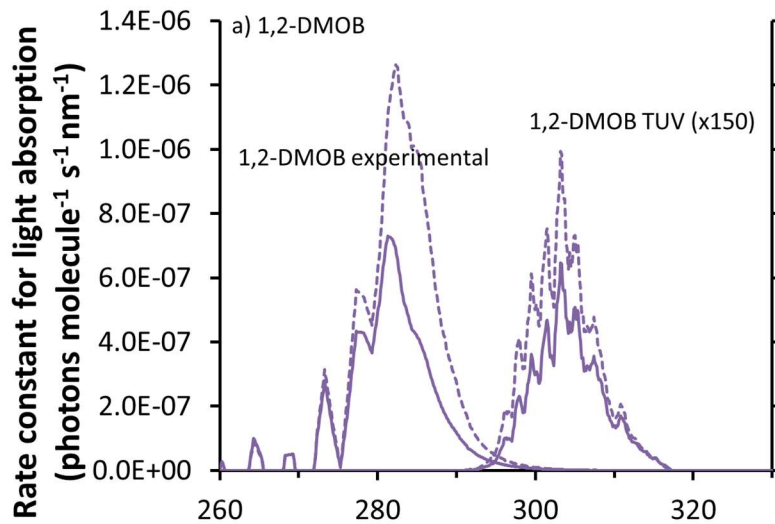


Supplemental Figure S14. Light absorbance spectra for DMOB isomers. Measured and modeled spectra for 1,2-, 1,3-, and 1,4-DMOB. For each isomer, solid black lines are the measured absorbance spectra in aqueous solution; solid and dashed colored lines are the aqueous and air-ice interface spectra estimated using molecular modeling (right axis); dashed black lines show the air-ice interface absorbance values predicted by combining

the measured aqueous absorbance spectra with the modeling results (see text for details). Modeled absorbance values (right axis) are arbitrary and not intended to correspond to actual molar absorptivities.



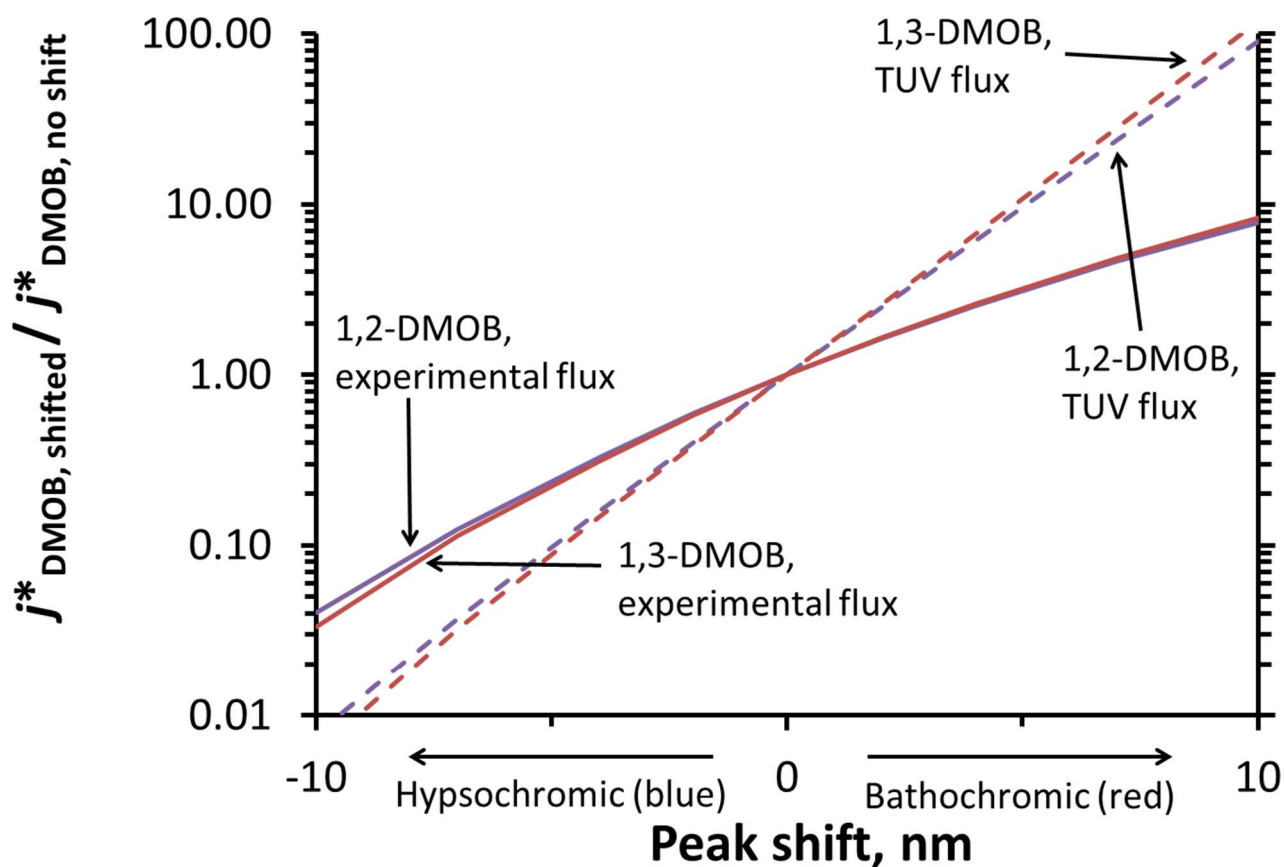
Supplemental Figure S15. Linear decomposition analysis for DMOB isomers. Linear Decomposition Analysis for the $\lambda_{predictions}$ for the three DMOB isomers. Bars and values represent the contributions of the phenyl ring (C_6H_4) and methoxy group (OCH_3) to the predicted excitation wavelength ($\lambda_{Decomposed}$) for 1,2- (top), 1,3- (middle) and 1,4-DMOB (bottom) in solution (blue) and at the air-ice interface (cyan).



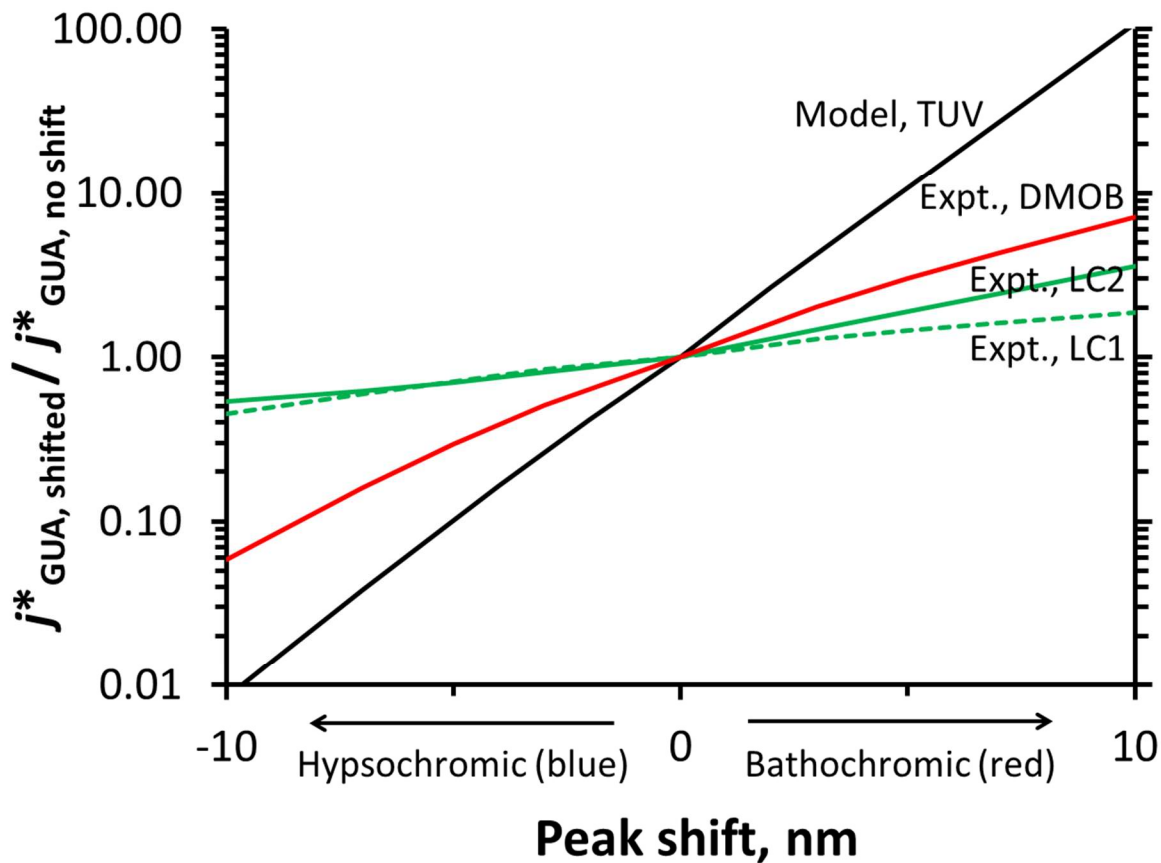
Supplemental Figure S16. Action spectra for DMOB light absorbance. Action spectra for light absorbance, determined for each DMOB isomer by multiplying the aqueous (solid lines) or predicted air-ice interface (dashed lines) molar absorptivity by the experimental or Summit conditions photon flux at each wavelength. Results are given at 1 nm resolution. The value at a given wavelength was determined as

$$\frac{2303}{N_A} I_\lambda \varepsilon_\lambda$$

where 2303 is a factor for units and base conversion ($1000 \text{ cm}^3 \text{ L}^{-1}$), N_A is Avogadro's number ($6.022 \times 10^{23} \text{ molecules mol}^{-1}$), I_λ is the photon flux at each wavelength ($\text{photons cm}^{-2} \text{ s}^{-1}$), and ε_λ is the wavelength-dependent molar absorptivity for each DMOB ($\text{M}^{-1} \text{ cm}^{-1}$). The area under each curve is the overall rate constant for light absorbance; these are tabulated in Table S4. For 1,2- and 1,3-DMOB, the Summit conditions rate constants have been scaled for readability.

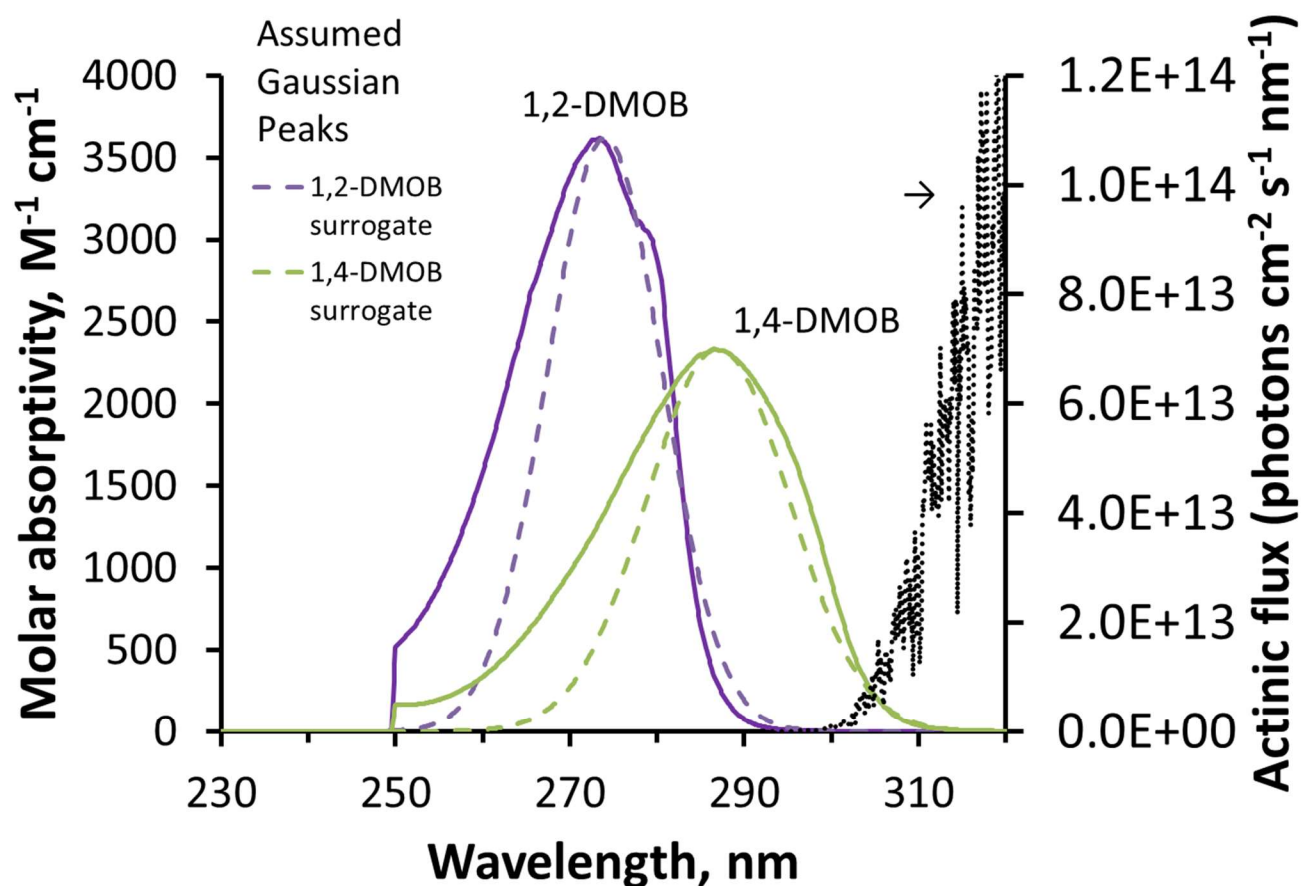


Supplemental Figure S17. Photodegradation rate constant ratios for shifted absorbance curves. Predicted changes in photodegradation rate constants (j^*_{DMOB}) for 1,2- and 1,3-DMOB due to shifting of absorbance relative to the unshifted value where the peak is centered at 280 nm. Rate constants were estimated using calculated quantum yields, aqueous absorbance spectra shifted hypsochromically (towards shorter wavelengths) or bathochromically (towards longer wavelengths), and either experimental photon fluxes (solid lines) or the TUV-modeled actinic flux for midday on the summer solstice at Summit, Greenland (dashed lines). See Figure 4 for the equivalent figure for 1,2- and 1,4-DMOB.

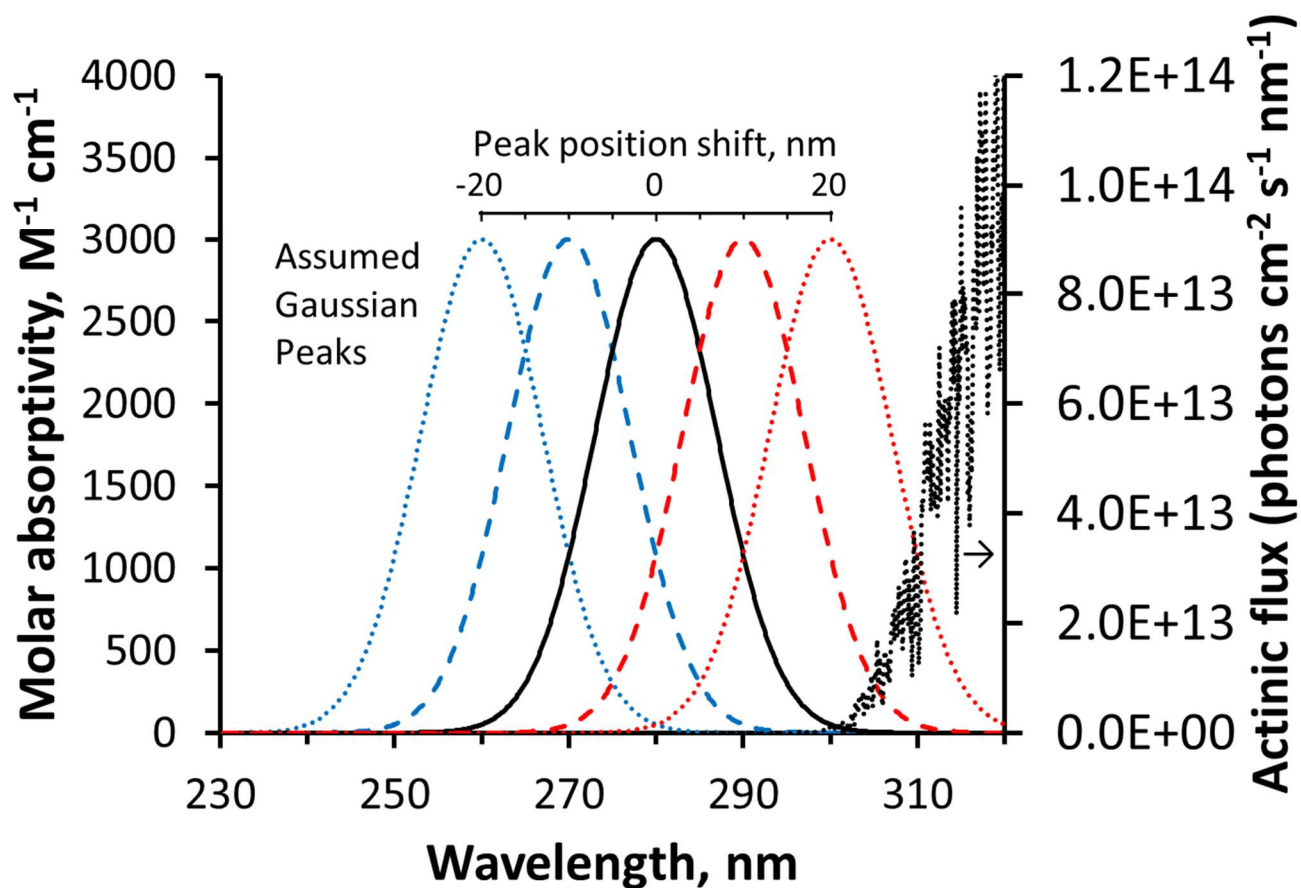


Supplemental Figure S18. Guaiacol photodegradation rate constants for various illumination conditions.

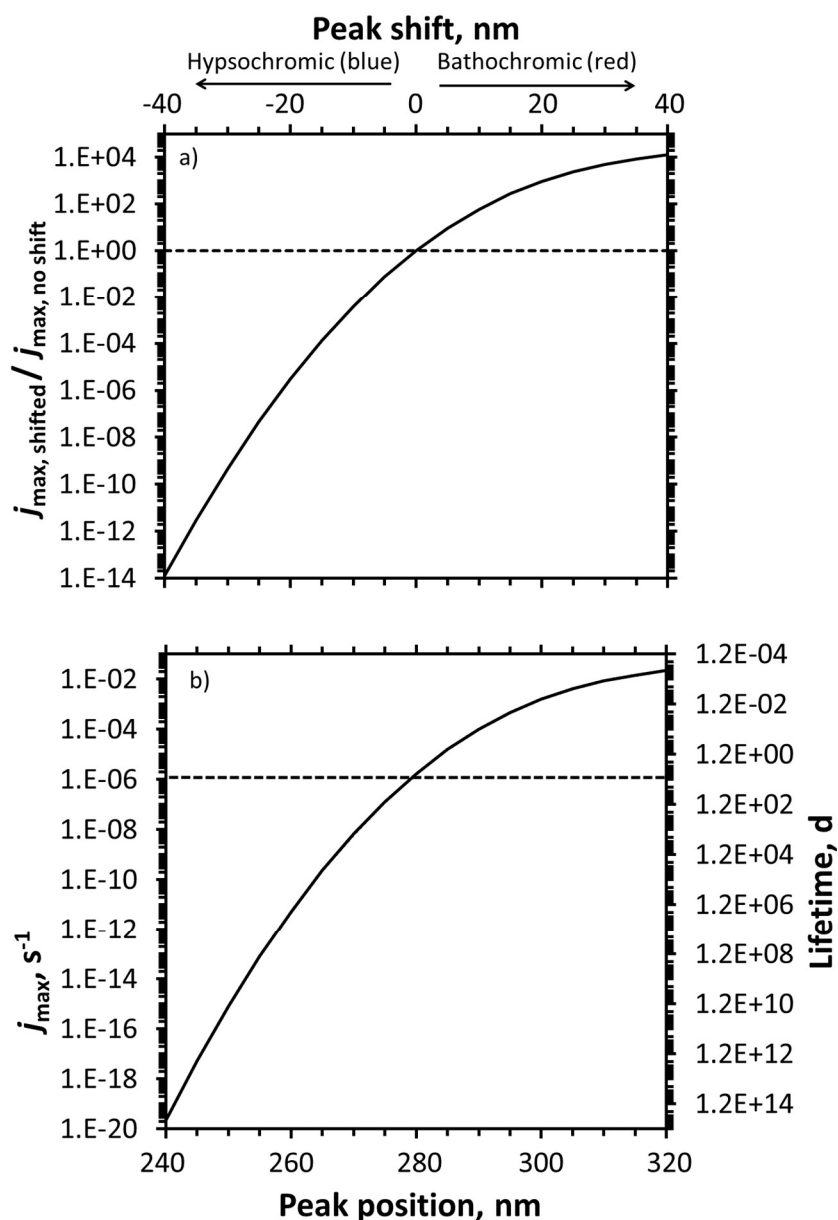
Absorbance shift impacts on calculated guaiacol photodegradation rate constants under several photon flux conditions. The black line represents rate constants calculated using TUV-modeled photon fluxes for Summit, Greenland at noon on the summer solstice; the red line uses the photon fluxes for experiments in this work; the green lines were calculated using the two experimental light conditions used in our previous guaiacol work (Hullar et al. 2020). The difference in photon fluxes between the solid red (DMOB) and green (LC2) lines is due to changing the cover material for the sample beaker: the current DMOB work uses a nylon film, while the previous LC2 guaiacol work used a polyethylene film.



Supplemental Figure S19. Absorbance spectra for DMOBs compared to assumed Gaussian peaks. Measured absorbance spectra and assumed Gaussian peaks for 1,2- and 1,4-dimethoxybenzene. Solid lines are the measured aqueous absorbance spectra, and the dashed lines are the Gaussian distributions chosen to approximate the measured spectra. The 1,2-DMOB and 1,4-DMOB surrogates have peak locations, standard deviations, and peak heights of 274 and 287 nm, 6.6 and 8.3 nm, and 368 and 2335 $M^{-1} cm^{-1}$ respectively. Black dashed line (right axis) represents the TUV-modeled actinic flux for Summit, Greenland.

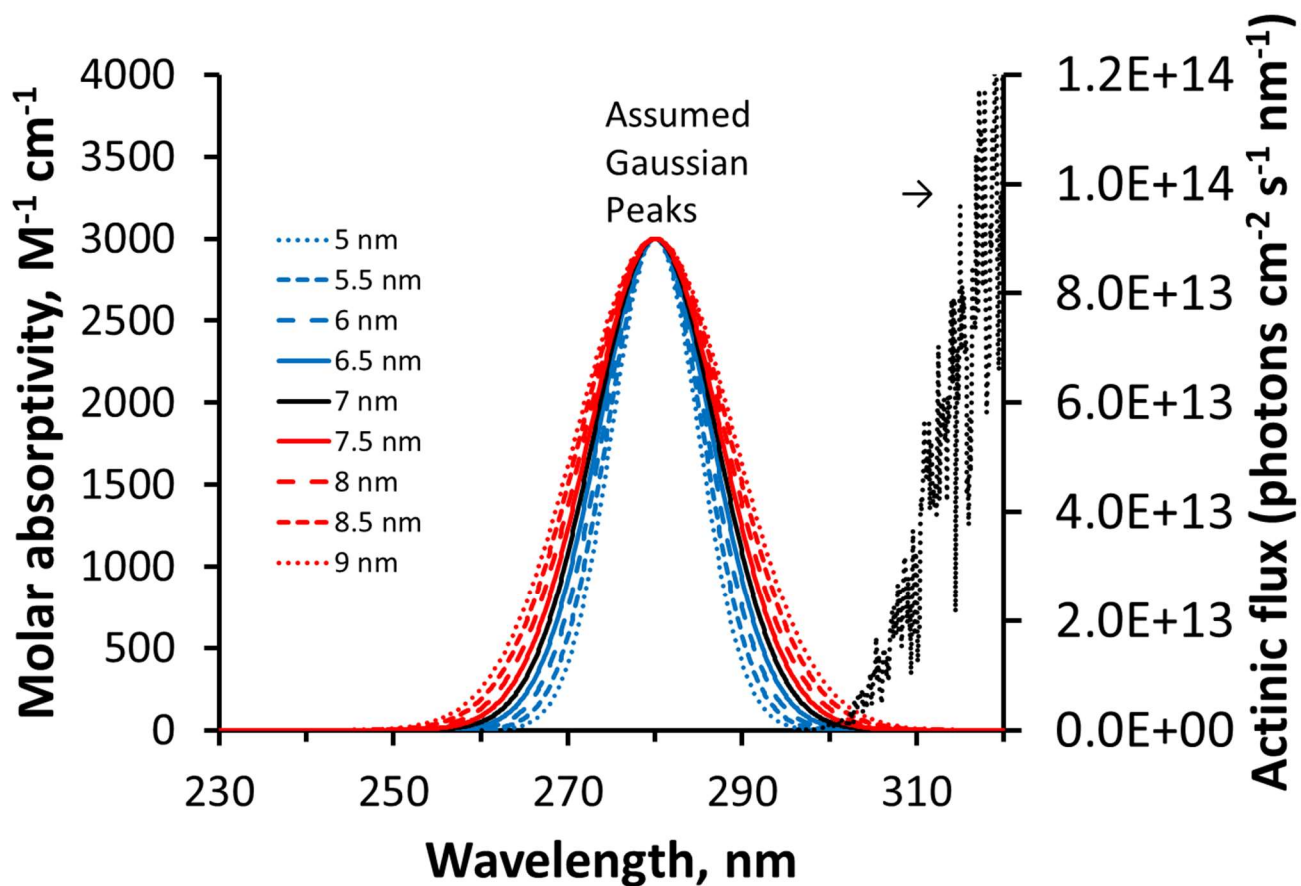


Supplemental Figure S20. Model compound absorbance spectra for various peak locations. Hypothetical model compound peak location with various position shifts. The solid black line represents the default center position of the assumed Gaussian peak (280 nm, standard deviation 7 nm, peak height $3000 \text{ M}^{-1} \text{ cm}^{-1}$), while blue and red lines show hypsochromically and bathochromically shifted peak locations, respectively. The black dashed line (right axis) represents the TUV-modeled actinic flux for Summit, Greenland.

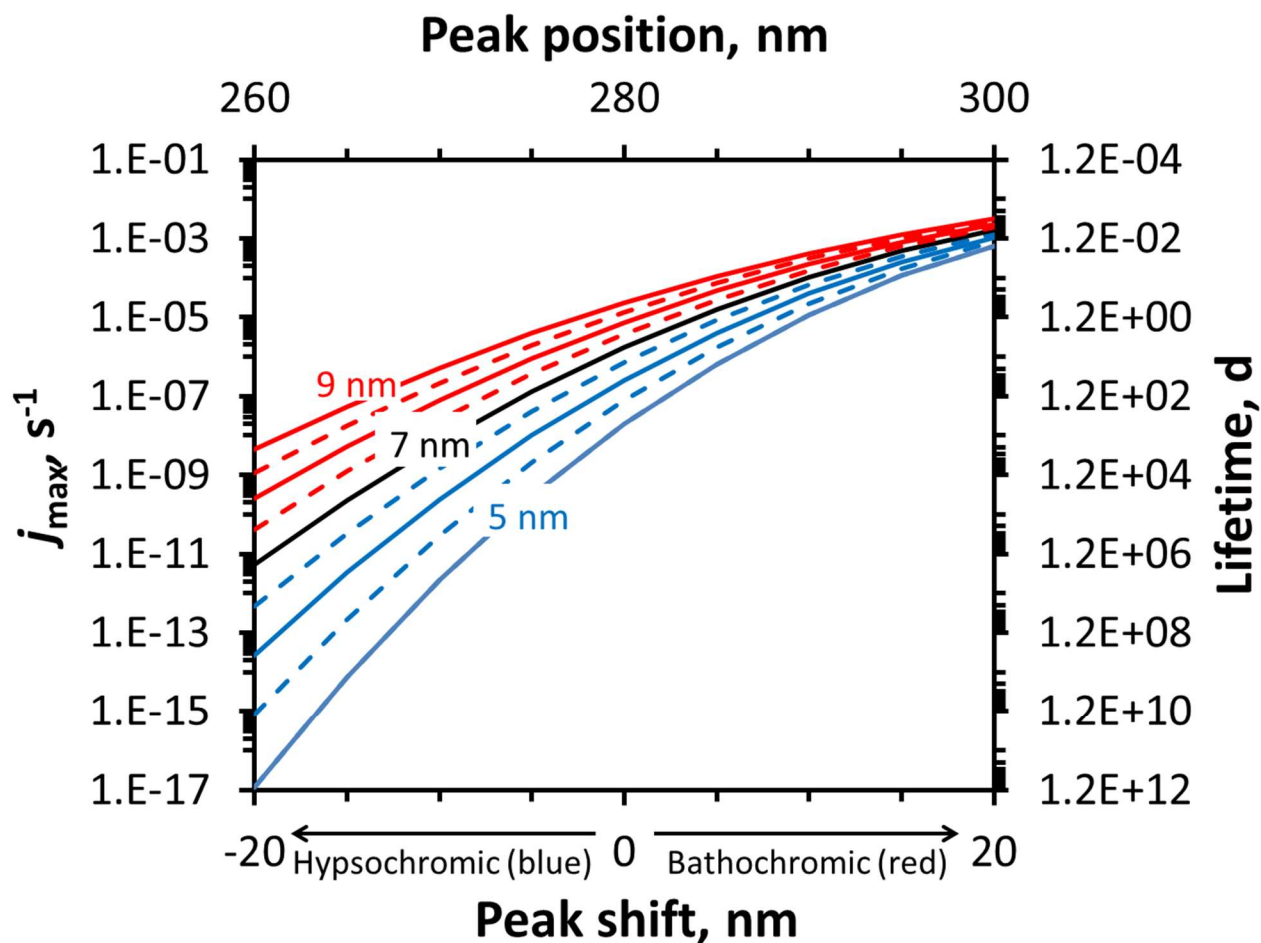


Supplemental Figure S21. Model compound photodegradation rate constants for various peak locations.

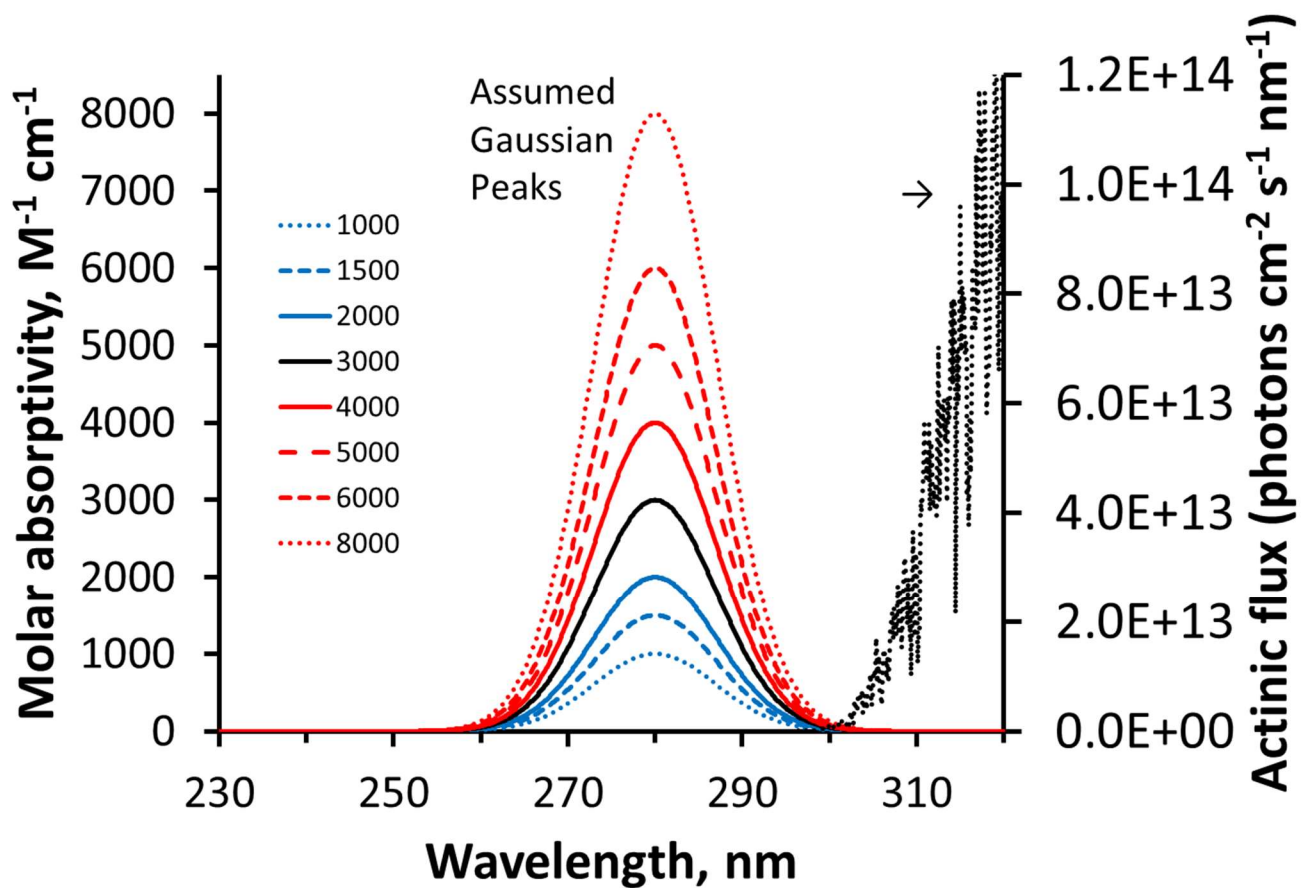
Predicted changes to photodegradation rate constants (j_{\max}) and the corresponding lifetimes resulting from absorbance shifts for a hypothetical model compound. Rate constants (j_{\max}) and lifetimes were calculated using an assumed quantum yield of 1, modeled actinic flux for Summit conditions, and an assumed Gaussian absorbance spectrum (peak molar absorptivity $3000 \text{ M}^{-1} \text{ cm}^{-1}$, standard deviation of 7 nm) with varying peak positions. a) Ratio of shifted to unshifted j_{\max} for varying hypsochromic (blue) or bathochromic (red) absorbance shifts. b) Calculated rate constants (j_{\max}) and lifetimes at various peak positions.



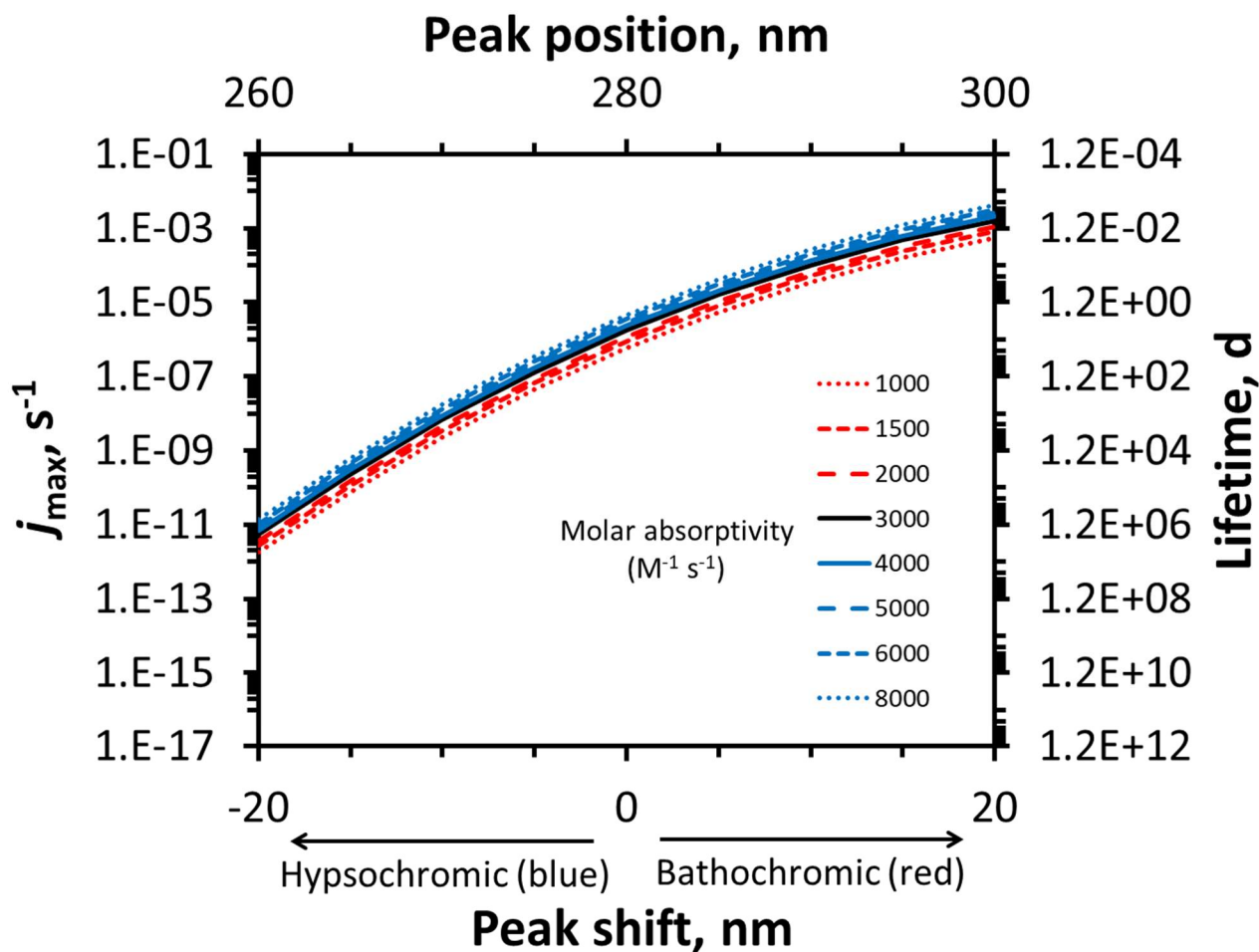
Supplemental Figure S22. Model compound absorbance spectra for various peak widths. Assumed absorption spectrum for a Gaussian hypothetical model compound showing baseline peak width (black line, standard deviation 7 nm) and various other peak widths (red and blue lines). Black dashed line (right axis) represents the TUV-modeled actinic flux for Summit, Greenland.



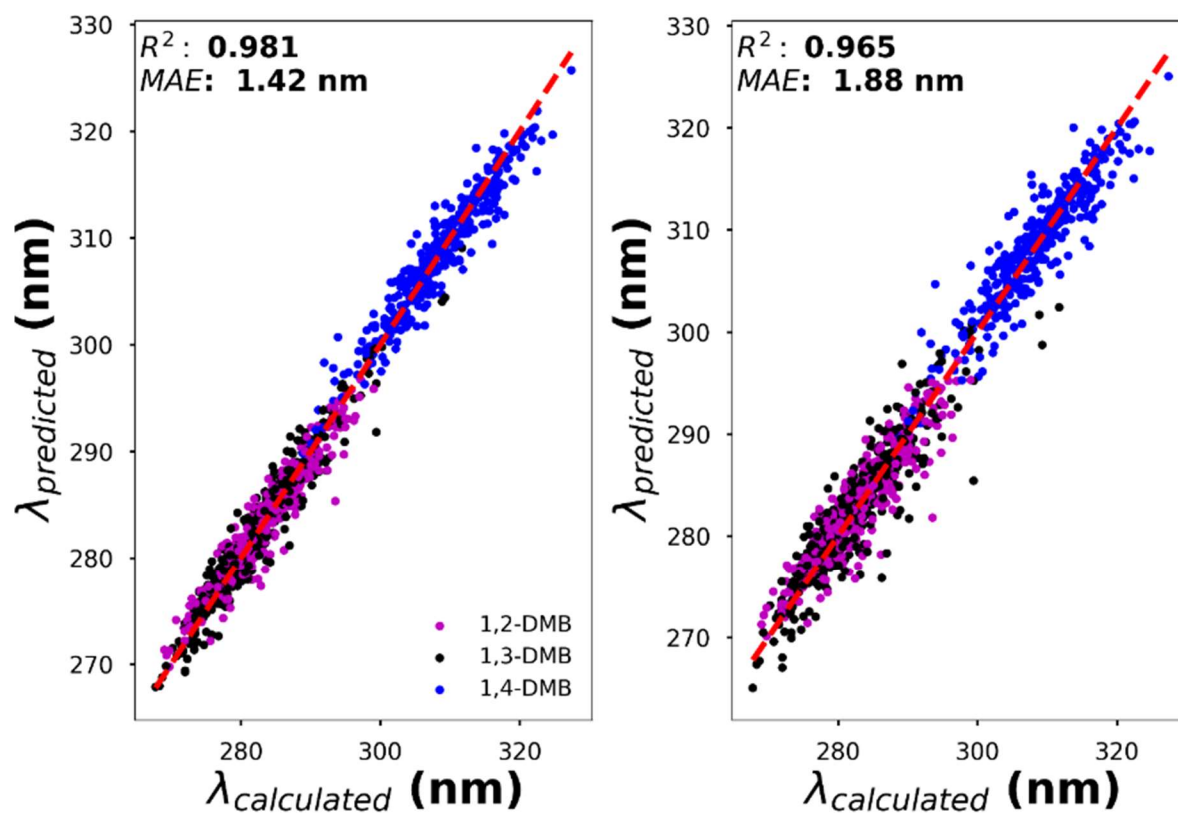
Supplemental Figure S23. Model compound photodegradation rate constants for various peak widths. Predicted changes to photodegradation rate constants and photochemical lifetimes resulting from variations in peak width (represented by various standard deviations of an assumed Gaussian absorbance spectrum) for a hypothetical model compound. The solid black line shows the baseline peak width (7 nm), while the red and blue lines show the rate constants and lifetimes for various peak widths and shifts.



Supplemental Figure S24. Model compound absorbance spectra for various molar absorptivities. Assumed absorption spectra for a Gaussian hypothetical model compound showing baseline peak height (black line, molar absorptivity = $3000 M^{-1} cm^{-1}$) and various other molar absorptivities (red and blue lines). The black dashed line (right axis) represents the TUV-modeled actinic flux for Summit conditions.



Supplemental Figure S25. Model compound photodegradation rate constant for various molar absorptivities. Predicted changes to photodegradation rate constants and photochemical lifetimes resulting from molar absorptivity changes for a hypothetical model compound. The solid black line shows the baseline peak height (molar absorptivity = $3000 \text{ M}^{-1} \text{ cm}^{-1}$), while the red and blue lines show the rate constants and lifetimes for various molar absorptivities and shifts.



Supplemental Figure S26. Machine learning parity plots. Parity plots for our unified machine learning model for the three DMB isomers. The R^2 and MAE are computed from the average R^2 and MAE from the 5-fold cross validation scheme. During each fold of the cross-validation scheme, a total of 888 frames were used in the training, 222 frames were used in the testing.

References

Hullar, T., F. C. Bononi, Z. K. Chen, D. Magadia, O. Palmer, T. Tran, D. Rocca, O. Andreussi, D. Donadio and C. Anastasio: Photodecay of guaiacol is faster in ice, and even more rapid on ice, than in aqueous solution, *Environmental Science-Processes & Impacts*, 22(8), 1666-1677, doi: 10.1039/d0em00242a, 2020